

**ALMA MATER STUDIORUM – UNIVERSITÀ DI BOLOGNA
CESENA CAMPUS**

**DEPARTMENT OF ELECTRICAL, ELECTRONIC AND INFORMATION ENGINEERING
“Guglielmo Marconi - DEI”**

**SECOND CYCLE DEGREE IN BIOMEDICAL ENGINEERING
*Class: LM-21***

**DEVELOPMENT OF POLY(ESTER AMIDE)S
BASED MEMBRANES WITH ANTIBACTERIAL
PROPERTIES**

**Graduation Thesis in
SMART MEDICAL IMAGING**

Supervisor
Professor Cristiana Corsi

Candidate
Alessio Di Serafino

Co-Supervisor
***Professor Ana Clotilde Amaral Loureiro
da Fonseca***

Academic Year 2022/2023

A Nonna Mirella...

Abstract

The present study focuses on the design and characterization of electrospun membranes embedding silver sulfadiazine (AgSD), intended to be used as advanced wound dressings.

The polymers used for the preparation of the membranes were poly(ester amide)s based on L-phenylalanine (PEA-Phe), that were obtained from the solution polycondensation between a bis- α -(L-amino acid)- α , ω -alkylene diesters (BAAD) and an activated ester of a dicarboxylic acid. After, the PEA-Phe were subjected to electrospinning for the obtainment of the membranes. For the embedding of AgSD, this was dissolved in the PEA-Phe solution that was subjected to electrospinning.

The membranes were then subjected to a thorough characterization in terms of their morphology, surface hydrophilicity, mechanical properties, *in vitro* cytotoxicity and antibacterial activity against *Escherichia coli* (*E. coli*) and *Staphylococcus aureus* (*S. aureus*). The membranes showed to have individualized fibers, but some with few defects. The membranes showed a hydrophobic surface, with contact angles higher than 90 °. In what respects the mechanical properties, the membranes showed properties, especially in terms of capacity of being stretched. The *in vitro* cytotoxicity tests showed that the membranes are non-cytotoxic to fibroblasts. In what concerns the antibacterial tests, unfortunately, the results showed that the membranes embedding AgSD did not present any antibacterial activity.

This study lays the foundation for further exploration to refine and optimize wound care materials, with particular attention to the

challenges encountered and opportunities for improvement in antimicrobial efficacy. The multidisciplinary approach adopted provides a detailed overview of the design and characterization of electrospun membranes, paving the way for future developments in the field of advanced wound dressings.

Contents

Contents	7
1 Introduction	10
1.1 Contextualization of the problem	10
1.2 Research Objectives	11
1.3 Relevance of the Thesis Work.....	11
2 Literature Review	13
2.1 Wound Healing	13
2.2 History of Wound Dressings	14
2.2.1 Wet revolution of the 60s and 70s & Moisture Healing from 80s	15
2.2.2 Dressings in the 90s and 21st century	15
2.3 Characteristics of Optimal Wound Dressings	16
2.4 Biomaterials in Wound Dressings	17
2.4.1 Materials for Wound Dressings with Antimicrobial Properties.....	19
2.4.2 Materials for Wound Dressings: Poly(Ester Amide)s ...	23
2.5 Fabrication Techniques for WD	28
2.5.1 Solvent Casting	28
2.5.2 3D Printing.....	30
2.5.3 Electrospinning (ES)	30
2.5.4 ES Parameters	33
3 Materials and Methods	37
3.1 Synthesis of the PEAs	37
3.1.1 Synthesis of the bis- α -(L-amino acid)- α , ω -alkylene diesters (BAADs)	37
3.1.2 Synthesis of the PEAs	39
3.2 Mats Preparation by Electrospinning-	41
3.3 Characterization Techniques	42
3.3.1 Nuclear Magnetic Resonance (NMR) Spectroscopy	42
3.3.2 SEC Analysis	43

3.3.3	Thermal Analysis	43
3.3.4	Scanning Electron Microscopy (SEM)	44
3.3.5	Contact Angle Analysis	44
3.3.6	Tensile tests.....	44
3.3.7	<i>In vitro</i> Cytotoxicity Tests.....	45
3.3.8	Antimicrobial test.....	45
4	Results & Discussion.....	47
4.1	BAAD Characterization	47
4.1.1	¹ H NMR Spectroscopy Analysis of the BAAD.....	47
4.1.2	Thermal analysis for BAAD.....	48
4.2	Characterization of the PEAs	49
4.2.1	¹ H NMR Spectroscopy Analysis of the PEAs.....	49
4.2.2	Molecular weight distribution of the PEAs	51
4.2.3	Thermal Analysis of the PEAs.....	52
4.3	ES Membranes Characterization	53
4.3.1	Morphology of the membranes	55
4.3.2	¹ H NMR spectroscopy analysis to the membrane	56
4.3.3	Contact Angle	57
4.3.4	Thermal Analysis for ES membranes	58
4.3.5	Tensile Tests	60
4.3.6	<i>In vitro</i> Cytotoxicity Tests.....	62
4.3.7	Antimicrobial Tests	63
5	Conclusions	66
6	Future Developments.....	67
	List of Figures	69
	List of Tables	71
	Bibliography.....	73
	Acknowledgments	79

1 Introduction

1.1 Contextualization of the problem

Effective wound management is a major challenge in medicine and requires advanced solutions to promote rapid healing and avoid complications such as infection. Most wound dressings (WD) that are used are the traditional ones that only act as a physical barrier between the wound and the surroundings. Especially in non-healing wounds, the development of a WD that can eliminate bacteria in the wound and at the same time promote tissue regeneration is of utmost importance. Thus, ideally, the WD should present antibacterial activity and should degrade as the new tissue is formed.

Electrospun membranes made from polymers, both natural and synthetic, are highly desirable because they have: (i) the ability to mimic the structural features of extracellular matrix (ECM), (ii) high surface to volume ratio, (iii) highly interconnected porous structure and (iv) the ability to incorporate active agents. Some of the polymers used in the electrospinning process do not allow to have the membranes with good mechanical properties to be used as WD, others do not have moieties in their structure that allow the enhancement of cell-materials interaction, and others release acid by-products during degradation, contributing to the inflammation of the surrounding tissues. To overcome some of the disadvantages presented by the currently used polymers in the development of WD by electrospinning, in this work, α -amino acid based poly(ester amide)s (AAA-PEAs) were used. These polymers gather in the same entity the best properties of polyesters and polyamides, with additional advantages being brought by the presence

of the α -amino acid. Also, they offer the possibility of being synthesized with a variety of structures, allowing the easy tailoring of properties.

1.2 Research Objectives

The main objective of this research was the design and development of AAA-PEA-based electrospun membranes embedding an antibacterial agent, that could be potentially used in the creation of advanced WD with antibacterial properties. To achieve this main objective, specific objectives were considered:

- Synthesis of AAA-PEAs by solution polycondensation, and optimization of the reaction conditions to obtain AAA-PEAs with the suitable molecular weight to be subjected to the electrospinning process;
- Optimization of the electrospinning process of AAA-PEAs in order to obtain membranes with individualized fibers and, ideally, free of defects;
- Characterization of the membranes in terms of their physical characteristics, along with their *in vitro* cytotoxicity and antibacterial activity.

1.3 Relevance of the Thesis Work

This work aims to explore new perspectives for the design of AAA-PEA-based membranes with antibacterial properties. The objective is to investigate the potential for the development of membranes that can make a significant contribution to the biomedical field by utilizing the intrinsic properties of AAA-PEAs. This study intends to evaluate the feasibility of developing more advanced WD in the hope that they will

offer significant improvements over currently available options. The work contributes to a possible innovation in the field of biomedical materials and contributes to the growing understanding of the applications of AAA-PEAs in the context of WD.

2 Literature Review

Adults and the elderly who suffer skin damage face significant challenges, as the ability of the dermis to regenerate spontaneously is limited and often results in permanent scarring. The conventional approach to treating such lesions, which relies on the use of traditional medications such as sterile dressings, gauze and antimicrobial creams, has proven inadequate when it comes to managing significant skin tissue loss.

To address this problem, it is essential to integrate the use of polymeric materials for dressings into the therapeutic approach. These particular materials represent innovative solutions that contribute significantly to the repair and healing of skin tissue over time and provide fundamental support, particularly in cases of severe injury [1].

2.1 Wound Healing

Wounds, especially chronic or complex wounds, require a multidisciplinary approach using innovative materials. Chronic wounds occur when wound healing is delayed, unlike acute wounds. The main difference between the two lies in the chemical environment of the wound: while acute wounds follow a controlled healing sequence, chronic wounds are often associated with bacterial infections that prevent the formation of new blood vessels. This represents a serious obstacle to the healing process and leads to imbalances in its phases. Chronic wounds also have a high level of inflammatory substances and a lack of growth factors. They also differ from acute wounds in terms

of the local pH value: acute wounds are slightly acidic, while chronic wounds have an alkaline environment [2].

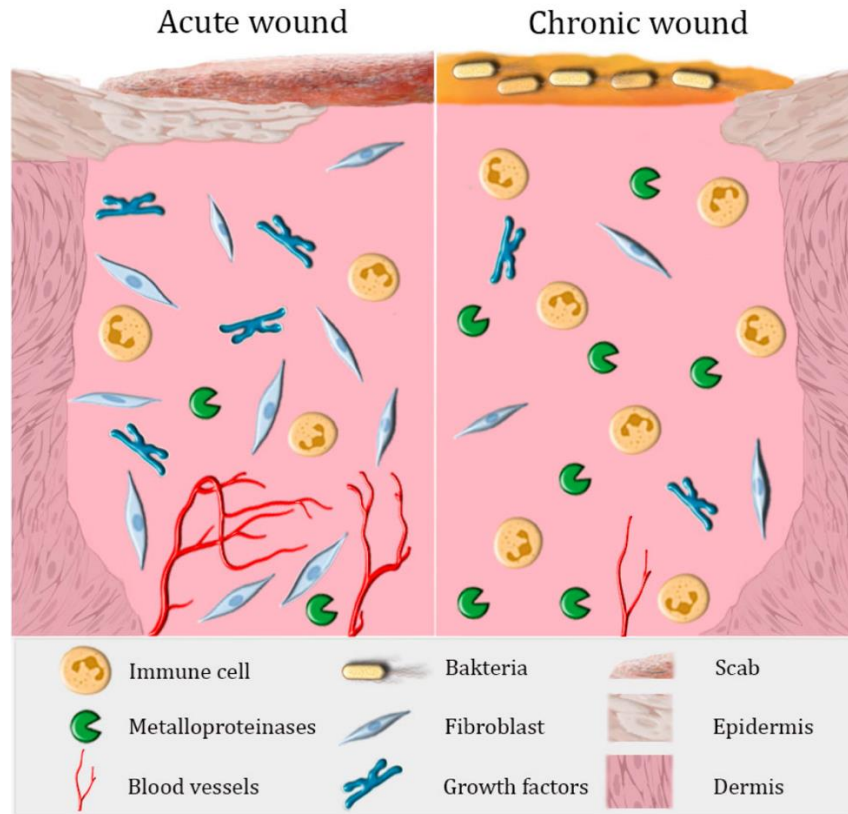


Figure 1 Schematic comparison of chronic and acute wound microenvironment [3].

The need for advanced materials is further enhanced by the increasing prevalence of bacterial infections associated with chronic wounds, which can impair healing and lead to serious clinical consequences.

2.2 History of Wound Dressings

Wound treatment has evolved over the millennia from traditional, ancient practices to advanced, scientifically-based therapies. For thousands of years, wound care has included practices ranging from magical spells to lotions and ointments [3]. The use of dressing materials such as feathers, gauze and compresses of various types were

primarily used to protect, absorb and create a foundation for healing. However, these methods were often based on beliefs rather than scientific evidence and resulted in adherence that caused wound trauma, often accompanied by bleeding when the dressing was removed [4].

2.2.1 Wet revolution of the 60s and 70s & Moisture Healing from 80s

The real breakthrough in the field of wound care came in the 1960s, with Dr. Winter's ground breaking discoveries in the field of moist healing. This revolution was further consolidated in the 1970s when research showed that semi-occlusive wound coverage accelerated healing. These findings paved the way to understanding the importance of the moist environment in promoting cell migration and the healing process [3].

Since the 1980s, the development of WD has accelerated significantly growth, with a growing awareness of the importance of moist healing [5]. The dressing industry has undergone an evolutionary and innovative process, that has resulted in a wide range of interactive products that create a moist environment to promote healing [6]. These advances contributed to a true revolution in wound care in the early 1990s, with a variety of products and extensive scientific research on moist healing [7].

2.2.2 Dressings in the 90s and 21st century

The 1990s were a time of explosive innovation in wound care. The development of advanced dressing materials, such as soft silicones, silver dressings and collagens, represented a major breakthrough. New therapies such as negative pressure and the use of antimicrobial agents, have expanded the treatment options for highly draining wounds [3][8].

In the 21st century, despite the remarkable advances of the 1980s and 1990s, there has been continued technological progress in wound care. Nevertheless, wet-dry gauze has remained the common choice, emphasizing the need to educate clinicians about the available treatment options. The future will focus on exploring new parameters and chemicals in chronic wound fluids and tissues, emphasizing the importance of understanding their balance. The increasing use of antimicrobials in WD requires further research to fully understand the change in bacteria levels. Substances such as nitric oxide and 'smart' skin grafts promise new prospects in advanced wound management, while pain management is crucial, with dressings designed to reduce trauma on application and removal [3].

Today, clinical practice continues to benefit from this evolution, with modern dressings designed to meet specific healing needs and address a broader range of factors, including those related to the patient. However, despite the clear consensus among experts on the efficacy of wet healing, challenges such as financial constraints and lack of knowledge still limit the use of these advanced techniques in wound care [7].

2.3 Characteristics of Optimal Wound Dressings

The characteristics of the ideal WD, as shown in Figure 2, include the ability to maintain a moist environment around the wound, good gas permeability and removal of excess fluid. They must protect the wound from microorganisms, prevent dissection, reduce surface necrosis, stimulate cell growth and provide mechanical protection. These

materials must be easy to remove, biocompatible, biodegradable and elastic, and help to reduce the pain caused by the wound [1].

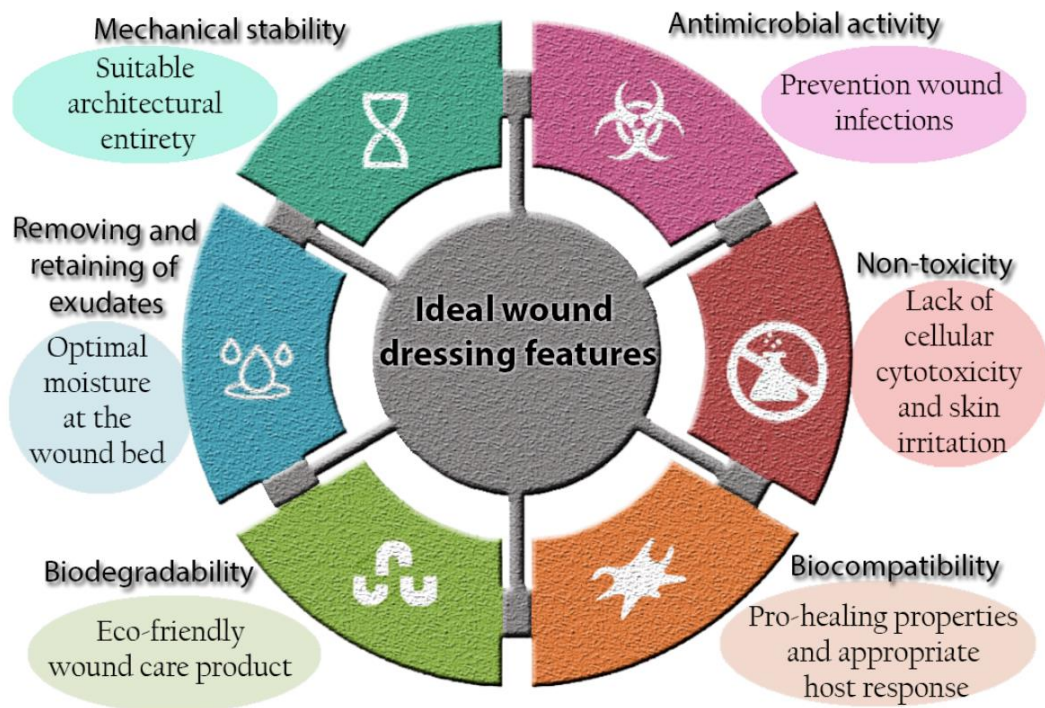


Figure 2 The features of the ideal WD [1].

2.4 Biomaterials in Wound Dressings

Polymers represent a versatile class of materials used in WD, and they can be processed in several forms, each one with unique characteristics. The most common WD based on polymers are:

- **Films** stand out for their thinness, flexibility, and transparency. They are indicated for uncontaminated, laser and superficial wounds. They offer advantages such as good gas permeability, impermeability to bacteria and fluids, easy monitoring thanks to transparency and less maceration and pain. However, they also

have disadvantages such adherence to the wound bed and impermeability to protein and drugs, which makes wound healing more complicated[1].

- **Foams**, consist of bilaminated layers of polyurethane, poly(ethylene glycol) (PEG) and silicone and are ideal for burns, chronic wounds, cavities and deep ulcers. Their advantages include high absorption capacity, maintenance of a moist environment, resistance to bacterial invasion and ease of application at low cost. However, they have disadvantages such as adhesion and the formation of an opaque layer, which makes wound monitoring more difficult [1].
- **Hydrogels**, composed of natural or synthetic polymers, are characterized by their high absorption capacity and their refreshing effect on skin wounds. They are suitable for various wounds and burns, and offer advantages such as high absorption capacity, easy of removal, reduction of pain and inflammation, low cost and easy administration. However, they also have disadvantages such as semi-transparency, gas and water permeability, poor bacterial barrier and sometimes limited mechanical stability [1].
- **Alginates**, made of alginate in the form of woven fibers, are suitable for surgical wounds and severe burns. Their advantages are their high absorbency, non-adherence, high mechanical stability, durability and easy removal with saline solution, which makes them a good bacterial barrier. However, they also have disadvantages such as high cost, unpleasant odor, complex handling and limited availability [1].

- **Hydrocolloids**, two-phase systems with iodine-immobilized starch, or dextran-PEG are indicated for chronic ulcers and burns. Their advantages are their high absorbency, easy removal with saline solution or sterilized water, lack of adhesion, and high density. However, they also have disadvantages such as variable antimicrobial activity, volumetric instability, excessive exudate loss, delayed healing with dextran hydrocolloids, as well as cloudiness, unpleasant odor and color changes [1].

2.4.1 Materials for Wound Dressings with Antimicrobial Properties

Polymers with antimicrobial properties were first developed in 1965 by Cornell [9] using derivatives of 2-methacryloxytrope. Since the 1980s, endogenous defense peptides and synthetic disinfectants have inspired the development of antimicrobial polymers. In 1984, the first cationic antibacterial polymers based on poly(vinylbenzylammonium chloride) were obtained and proved to be effective [10]. Some polymers have inherent antibacterial properties, while others can be designed to be activated during use [11]. The various methods used to incorporate antibacterial properties into polymers will be presented below.

2.4.1.1 Natural Polymers

Some natural polymers, such as chitosan and chitin, have inherent antibacterial properties [12]. Chitosan, which is obtained from the deacetylation of chitin, is biocompatible but only dissolves in acidic solutions, so its antibacterial activity is limited to acidic environments. [13][14]. Its limited solubility at pH above 6.5 reduces its antibacterial efficacy in neutral or alkaline environments. Although chitosan is widely used in biomedical applications, it is crucial to consider the

characteristics of the site of application to maximize its antibacterial benefits. Other biomacromolecules such as cellulose or starch need to be chemically modified to achieve antibacterial activity [10].

2.4.1.2 Synthetic Polymers

Synthetic polymers with antibacterial properties are a promising area of research in the fight against bacterial infections. Despite initial concerns about unwanted biological reactions, significant advances in synthesis techniques have paved the way for new materials with specific biological applications. One of the examples is a copolymer of maleic anhydride (MA) and divinyl ether (DVE) (DIVEMA), which is obtained by a cyclopolymerization reaction with in-chain pyran [10]. DIVEMA shows antibacterial activity against Gram-positive and Gram-negative bacteria, and fungi [15]. These polymers offer a wide range of applications, ranging from medicine to industry, and present innovative potential in the field of antibacterial agents.

In another study, copolymers comprising cationic monomers and alkyl-substituted polynorbornes were synthesized. These copolymers exhibited mild antibacterial activity against *Staphylococcus aureus* (*S. aureus*) and *Escherichia coli* (*E. coli*), with the efficacy being dependent on the hydrophobicity of the polymer. The study concluded that achieving a balance between hydrophobic and hydrophilic regions is more crucial than the overall charge density or global amphiphilicity for the polymer present antibacterial activity [16].

As with natural polymers, synthetic polymers can also be modified to introduce bacterial properties [10].

2.4.1.3 Modification of Synthetic and Natural Polymers with Antibacterial Effective Metals & Organic Compounds

The functionalization of polymer surfaces with metal ions or metal oxides, especially zinc, is an area of growing interest to impart antibacterial properties to polymers [10][17]. Zinc ions, which are known to inhibit amino acid metabolism and active transport in bacterial cells, are released from zinc oxide nanoparticles. These nanoparticles exhibit photocatalytic activity in the presence of light and generate reactive oxygen species (ROS), which contribute to the peroxidation of bacterial lipids, damage to nucleic acids, and oxidation of proteins [18]. In addition, the chemical and physical stability of zinc nanoparticles makes them popular modulators of the polymer matrix. The synthesis of zinc oxide modified nanostructures is carried out by various techniques, such as precipitation [19] and atom transfer radical polymerization (ATRP) [20], which allows fine control of the interactions between molecular fillers and the polymer matrix by simultaneously growing all polymer chains at the same rate. Such polymer modifications have shown excellent antibacterial properties, and open promising perspectives for applications in the development of wound care materials [10].

Among organic compounds, the modification of synthetic and natural polymers with fatty acids is an important field of research [10]. Fatty acids, which are produced by algae and plants to defend against pathogens, show antibacterial activity against various bacterial strains. The modification of polymers with oleic, linoleic and palmitic acids allows them to show activity against *E. coli* and *S. aureus* [21]. Furthermore, fatty acids such as decanoic and oleic can be used for the post-polymerization modification of polyurethanes, improving their

antibacterial activity against Gram-positive strains [22]. These modifications represent an interesting prospective for the development of polymeric materials with new functionalities and practical applications.

2.4.1.4 Silver Sulfadiazine & Curcumin

Silver sulfadiazine (AgSD) is considered an ideal antibacterial agent for burn wounds due to its bifunctional action [23]. The antibacterial properties of AgSD derive from the ability of the sulfonamide fraction to inhibit bacterial folate absorption and subsequent DNA synthesis [24]. In addition, the silver released from the AgSD binds to and disrupts the structure of bacterial DNA, preventing replication [25]. However, the performance of AgSD is limited by its poor water solubility. Consequently, current research focuses on nanotechnology methodologies to improve the effectiveness of AgSD. An example of this is the synthesis of AgSD particles modified with poly(N-vinyl-2-pyrrolidone) (PVP), which demonstrated notable antibacterial effects against several bacterial strains [26].

Curcumin, extracted from turmeric, demonstrates positive effects in WD through regulation of inflammation through inhibition of nuclear factor kappa-light-chain-enhancer of activated B cells (NF-(κ)B) and modulation of ROS [27]. In the proliferation phase, it promotes the migration of fibroblasts, the formation of granulation tissue and the deposition of collagen. During remodeling, curcumin enhances wound contraction by increasing the amounts of transforming growth factor beta (TGF- β) and stimulating fibroblast proliferation. These findings suggest the potential use of curcumin in WD, with the need to carefully

optimize doses to maximize benefits without compromising cellular safety [27].

In the context of the discussion on synthetic polymers with antimicrobial properties, there is the need to take a closer look at the panorama of advanced materials designed to improve wound healing. Poly(ester amide)s (PEAs) represent an interesting category in this area as they offer a unique combination of biodegradability and other tailored properties. Moving from the discussion of conventional synthetic polymers to PEAs, we are exploring a class of materials that provide a versatile platform for WD applications.

2.4.2 Materials for Wound Dressings: Poly(Ester Amide)s

In recent years, PEAs have gained considerable importance as an important family of biodegradable synthetic polymers.

2.4.2.1 PEAs Characteristics

PEAs incorporate both ester and amide bonds in their structure, combining the favorable biodegradability and solubility of polyesters with the excellent thermo-mechanical properties and biocompatibility of polyamides. Indeed, polyesters degrade under physiological conditions through the cleavage of the ester linkages, have better solubility in many organic solvents, and have better flexibility than polyamides. In turn, polyamides are known to have superior thermal and mechanical properties due to the formation of strong hydrogen bonds between the amide linkages of individual chains [28]. On the other hand, polyamides often require a prolonged period of time to degrade in the human organism, making them virtually non-degradable.

The combination of ester and amide bonds in the same polymer opens up new perspectives for the development of materials with different properties, such as thermomechanical characteristics and degradability, which are particularly relevant in biomedical applications [29].

PEAs based on α -amino acids combine the attractive properties of conventional PEAs with those resulting from the presence of the α -amino acid, such as enzymatic degradability, the improvement of cell-material interactions and the introduction of functional groups for the binding of drugs or peptides [30][31]. This improves the overall biodegradability of these polymers [32].

2.4.2.2 Synthesis of α -amino acids-based PEAs

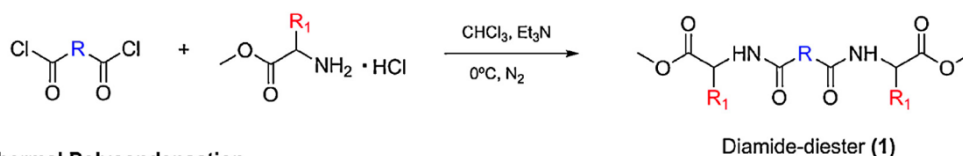
The methods currently used to synthesize this type of PEAs are melt polycondensation, interfacial polycondensation, and active solution polycondensation.

Melt polycondensation

The synthesis of PEAs through melt polycondensation involves the reaction of a diol with a diamide-diester, previously obtained by the condensation of a diacyl chloride with a α -amino acid methyl ester [28]. The process occurs in two stages, as shown in Figure 3. In the first, the diamide-diester is formed at low temperatures with the use of a base, usually triethylamine (Et_3N). Then, in the second stage, the purified diamide-diester is heated and subjected to a vacuum to aid condensation [33][34]. This method is industrially advantageous because it does not require post-synthesis treatments, but has disadvantages such as the need to purify the diamide-diester and high temperatures which can cause unwanted reactions [28]. Studies show that this approach has

resulted in PEAs with good yields and various properties, such as the ability to form films and fibers [33].

1) Formation of the diamide-diester



2) Thermal Polycondensation

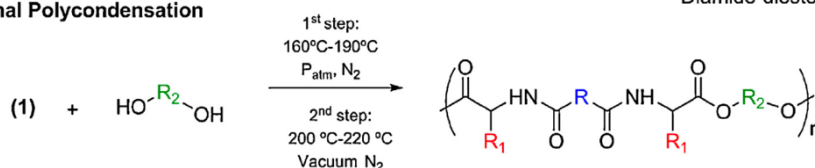
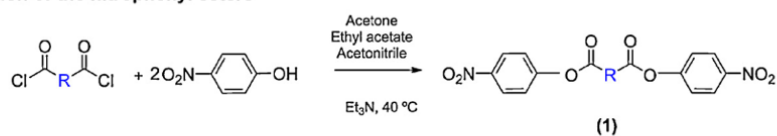


Figure 3 Synthesis of PEAs containing α -amino acids from a thermal polycondensation of a diol and a diamide–diester. R and R2, alkyl chain of variable length; R1, α -amino acid side chain [32].

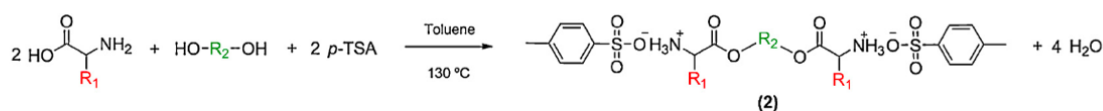
Solution Polycondensation

The synthesis of PEAs via solution polycondensation is a method developed to overcome the disadvantages of melt polycondensation reactions, such as unwanted side reactions due to high temperatures. This approach features moderate reaction conditions ($T < 80\text{ }^{\circ}\text{C}$ and atmospheric pressure), high polymerization rates and minimal side reactions, resulting in polymers with high molecular weights [28]. Polycondensation in solution involves the use of condensing agents or the activation of carboxyl groups, known as active solution polycondensation [31][35].

1) Preparation of the nitrophenyl esters



2) Preparation of bis- α -(L-amino acid)- α , ω -alkylene diesters



3) Solution Polycondensation

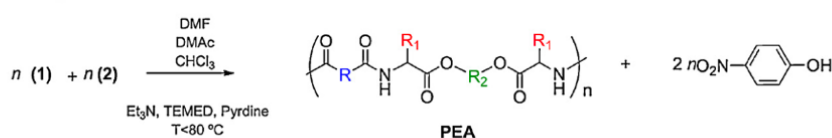


Figure 4 Solution polycondensation method for the preparation of α -amino acid-based PEAs. R and R_2 are aromatic or aliphatic chains of variable length and R_1 is the α -amino acid side chain [32].

The synthesis of PEAs via solution polycondensation comprises three main steps, as shown in Figure 4. Initially, bis- α -(L-amino acid)- α , ω -alkylene diesters (BAADs) are prepared through Fischer esterification between α -amino acids and diols, using *p*-toluenesulphonic monohydrate (*p*-TSA) as a catalyst and amino group protector. BAADs are obtained as salts to avoid unwanted reactions in free form. Subsequently, the carboxylic acid is activated via a good leaving group, such as *N*-hydroxysuccinimide (NHS), forming activated esters. Finally, the condensation reaction of the activated dicarboxylic acid with the BAAD occurs, to yield the PEA. This method is advantageous for obtaining PEAs with high molecular weight [31]. However, it also has some disadvantages; it requires high purity monomers to maintain a correct stoichiometric balance and obtain high molecular weight polymers [36]. Furthermore, thorough purification of the polymer is required to remove solvents and toxic byproducts [30].

Interfacial Polycondensation

Interfacial polycondensation is a rapid method that occurs at the interface between two immiscible phases, usually organic solvent/water. This occurs through the Schotten-Baumann reaction between a diacyl chloride reagent with compounds containing hydrogen atoms (OH, NH and SH) [31]. The selection of the organic solvent is critical, impacting multiple facets of the reaction and the characteristics of the resulting polymer. A base in the aqueous phase is vital to neutralize the produced hydrochloric acid. This is imperative to prevent the protonation of the amino group, making it non-reactive [37]. Effective stirring is indispensable to guarantee the dispersion of the two phases and the renewal of interfaces, augmenting the available surface area for the reaction [38].

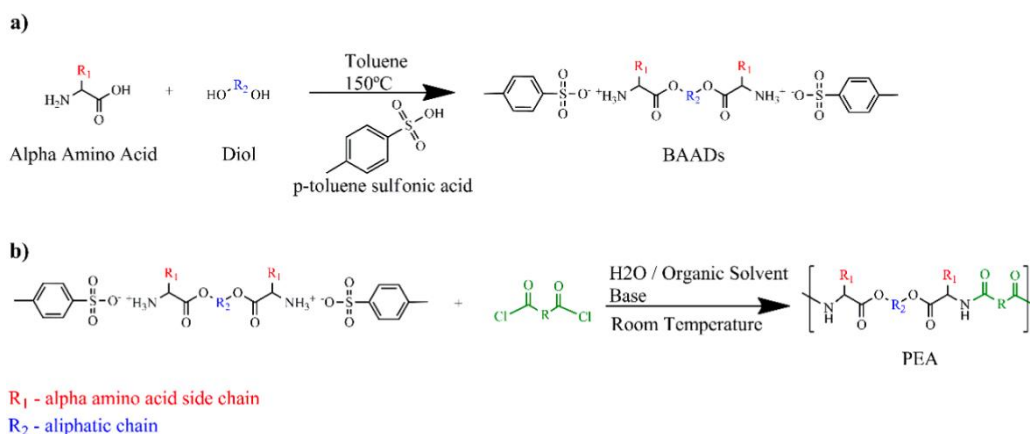


Figure 5 Synthesis of α -amino acid PEAs by interfacial polycondensation.

Figure 5 shows the two main steps of interfacial polycondensation. The first step of the synthesis involves the preparation of di-p-toluenesulfonic acid salts of BAADs by Fischer esterification between α -amino acids and diols, in presence of pTSA. Subsequently, the BAADs salts react with diacyl chlorides in the presence of a proton

acceptor [39]. Interfacial polycondensation is considered the most practical method for the synthesis of this type of PEAs since it is a fast reaction carried out at room temperature, avoiding unwanted reactions related to the use of high temperatures. However, hydrolysis of diacyl chloride may occur, causing chain termination and unit heterogeneity [40].

2.5 Fabrication Techniques for WD

The production of WD is a constantly evolving field in which various methods are used. Among the various techniques, electrospinning, solvent casting and 3D printing stand out.

2.5.1 Solvent Casting

Solvent casting is a widely used method for producing polymer films, known for its reliability and low costs. This is a very simple process that involves the solubilization of polymers and some additives (e.g. plasticizers), followed by film formation through solvent removal [41] [42]. In the context of wound healing, solvent casting offers transparency, porosity, cost-effectiveness and flexibility. However, some disadvantages should be noted such as the excessive use of solvent, the long drying phase and the limited adjustment of the film thickness [43].

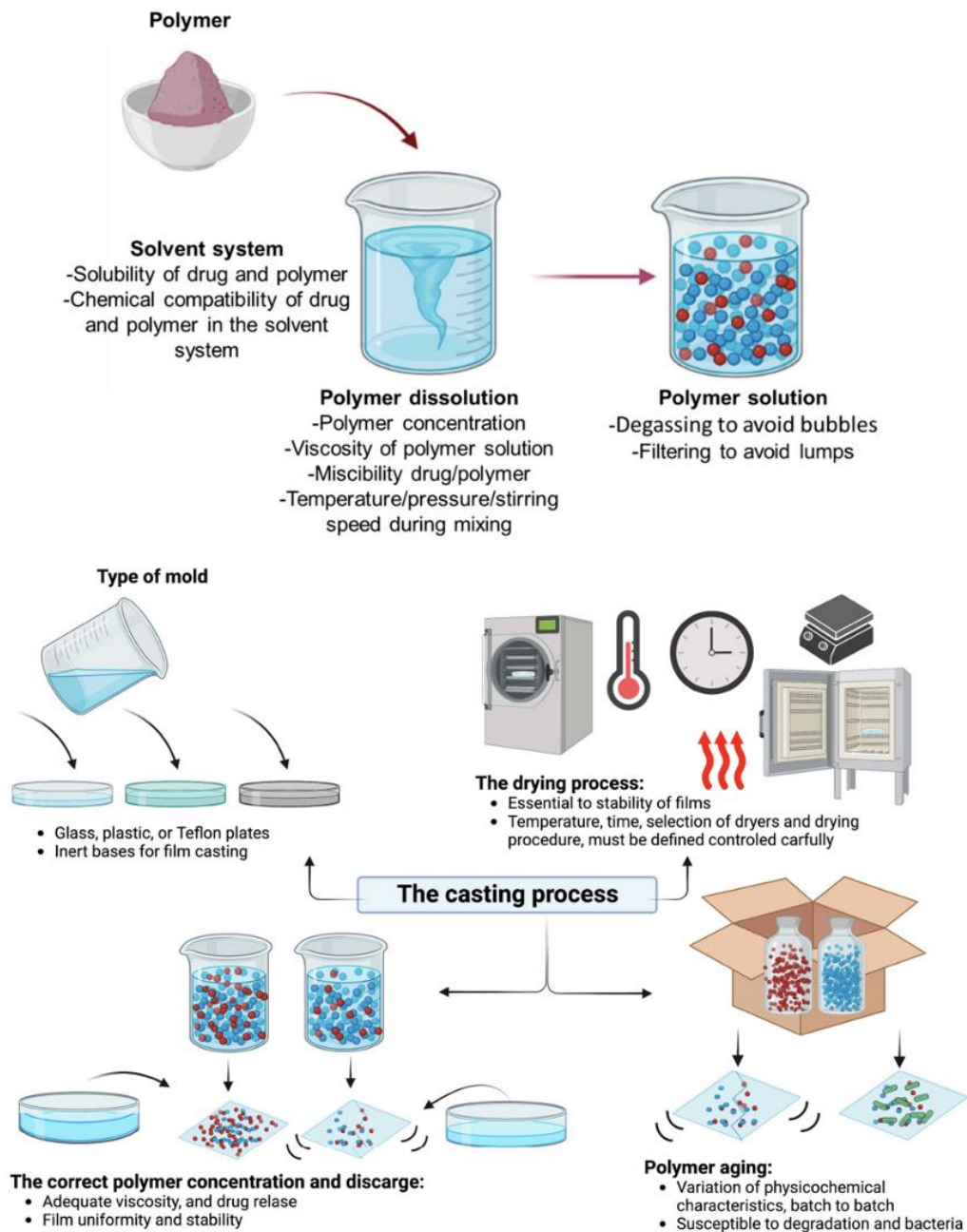


Figure 6 The solvent-casting process [41].

In the solvent-casting process (Figure 6), polymers, additives and active compounds are dissolved in a suitable solvent. This solution is then poured into a desired geometric shape. The choice of solvent, the formation of homogeneous solutions and the optimization of dissolution conditions are fundamental [41]. Then all the ingredients

that are dissolved in the solvent are poured onto a support. Subsequently, the material is dried, cut and packaged.

2.5.2 3D Printing

3D printing sets itself apart from WD production processing by enabling the customization of porosity by changing the degree of infill and creating tailored geometries. 3D printing enables precise control over the porosity and geometric configuration of the bandages, helping to improve the healing process. In addition, 3D-printed dressings enable the incorporation of layers of biomaterials and therapeutic agents, overcoming challenges that conventional dressings cannot [44].

2.5.3 Electrospinning (ES)

Electrospinning is a process by which very thin fibers are produced from a drop of liquid. The process uses a simple apparatus that includes a high-voltage power supply, a syringe pump, a small tube called a "nozzle" and a conductive surface to collect the fibers (Figure 7).

The working principle of electrospinning is as follows: the syringe pump pushes the liquid in a thin stream through the nozzle/spinneret. An electrical voltage is applied between the spinneret and the collector. This voltage creates a potential difference between the spinneret and the collector. The drop of liquid coming out of the spinneret is electrified by the electrical voltage. This leads to an electrostatic repulsion between electric charges of the same sign, causing the droplet to deform into a conical shape, the so-called "Taylor cone". An electrically charged jet projects from this Taylor cone. Initially, the jet

extends in a straight line, later it begins to undulate due to instabilities in its shape. As the jet lengthens and thins, it quickly cools and solidifies. This process leads to the formation of solid fibers which are collected on a collector [45].

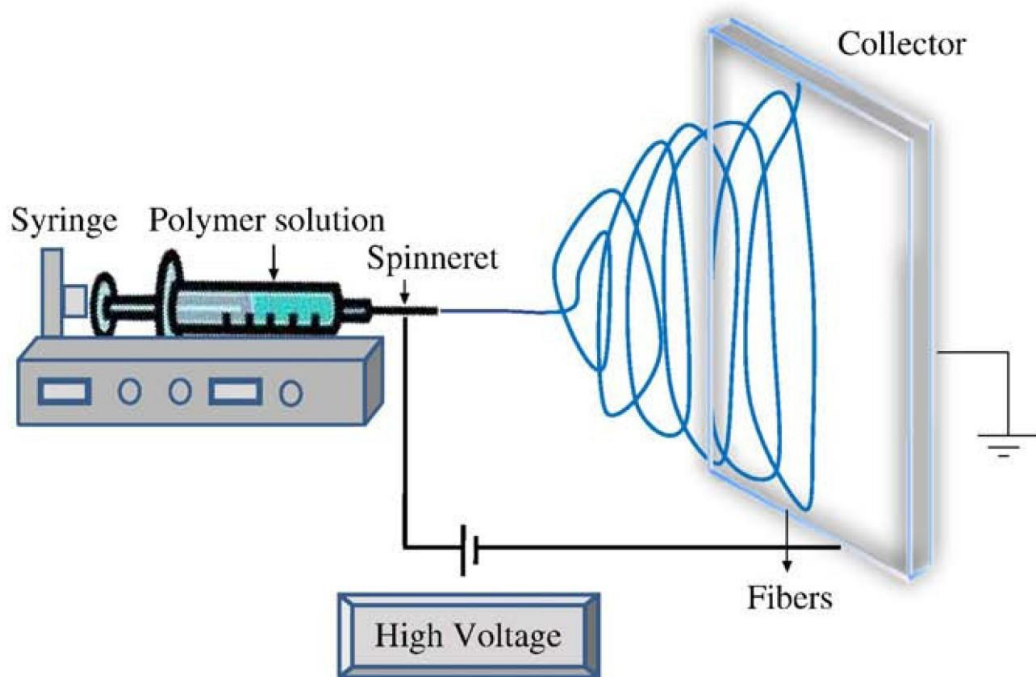


Figure 7 Schematic exemplification of the conventional ES process [45]

The Taylor's cone formation phenomenon can be best understood through an example involving the formation of Rayleigh jets from small drops of ethylene glycol suspended in an electric field.

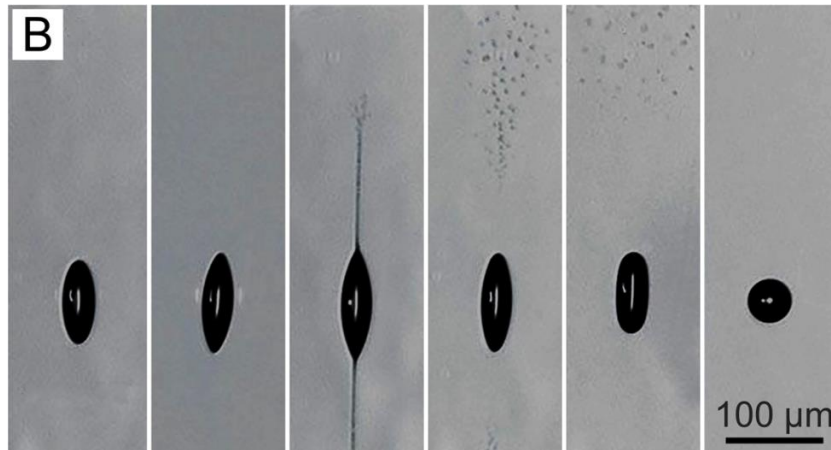


Figure 8 High-speed photographs showing the disintegration of a levitated droplet of ethylene glycol charged to the Rayleigh limit for the ejection of two jets [46].

In this experiment, a small drop of ethylene glycol is first injected into an environment in which an electric field is present. The drop has a spherical shape with a certain electrically charged radius. Over time, the droplet shrinks due to the evaporation of neutral molecules from the surface and its radius gradually decreases. When the radius of the droplet reaches a certain critical limit, known as the "Rayleigh stability limit", the droplet can no longer maintain its spherical shape and deforms into an ellipsoidal shape. During this deformation process, two sharp points form at the poles of the ellipsoid. Almost immediately after the formation of these points, two thin jets of liquid emerge from opposite points and move away from the original droplet, as shown in Figure 8. These jets break up into small droplets that are repelled away from the original droplet due to electrostatic repulsion. Over time, the jets and tips disappear, and the droplet returns to a spherical shape. This process of deformation, jet formation and return to spherical shape is a manifestation of the Taylor's cone and illustrates how a charged droplet can transform in an electric field and generate jets of liquid [47].

2.5.4 ES Parameters

The ES process is influenced by various parameters that determine the quality of the fibers obtained. These include the type and properties of the polymer, the properties of the solvent, the processing parameters (applied electric field, distance between needle and collector, and the flow rate), and the ambient conditions (temperature and humidity). By adjusting these parameters, it is possible to obtain fibers with different diameters, morphologies and electrospun mats with different pore sizes [45].

The influence of the applied electrical field on the fiber diameter is significant. Studies show that increasing the voltage above the critical threshold reduces the dimensions of the Taylor's cone and at the same time increases the velocity of the jet [48]. Flow rate is another crucial parameter that affects fiber diameter, pore size and bead formation. Maintaining a minimum flow rate is important to establish a balance between the discharged polymer solution and its replenishment. However, an excessive increase in flow rate can lead to the formation of beads or ribbon-like structures. The distance between the needle tip and the collector plays a crucial role in achieving high quality mats, as it influences the evaporation of the solvent and solution stretching [49].

Important solution parameters such as polymer concentration, solvent, viscosity, and conductivity, play a pivotal role in the ES process. Insufficient polymer concentration can lead to the formation of fragmented and beaded fibers, while increasing the concentration increases the viscosity, resulting in uniform, bead-free fibers. However, exceeding a critical viscosity level impedes the flow of the solution through the needle tip, and thus poses a challenge for production [49].

Optimal conductivity is crucial for the formation of the Taylor's cone and affects the fiber diameter, with higher conductivity values associated with smaller fiber diameters. Careful consideration of these solution parameters is essential for the success of ES process. Room conditions, such as temperature and humidity, affect fiber diameter and must be carefully controlled [50].

The choice of solvent is also critical. The boiling point is of fundamental importance as it must not be too low so that the solvent does not evaporate too abruptly, but also not too high so that it does not evaporate sufficiently before reaching the collector. The toxicity of the solvent must also be carefully checked [51].

2.5.4.1 ES Types

Electrospinning can be performed in different ways (Figure 9), each method having its own advantages and disadvantages. The simplest method consists of a single syringe, a pump, and a flat collector. This method allows the production of filled or unfilled fibers obtained from a single polymer or from mixtures of polymers soluble in the same solvent. As already mentioned, the adjustment of ES parameters allows the production of mats with specific properties and the incorporation of active compounds with control over their release.

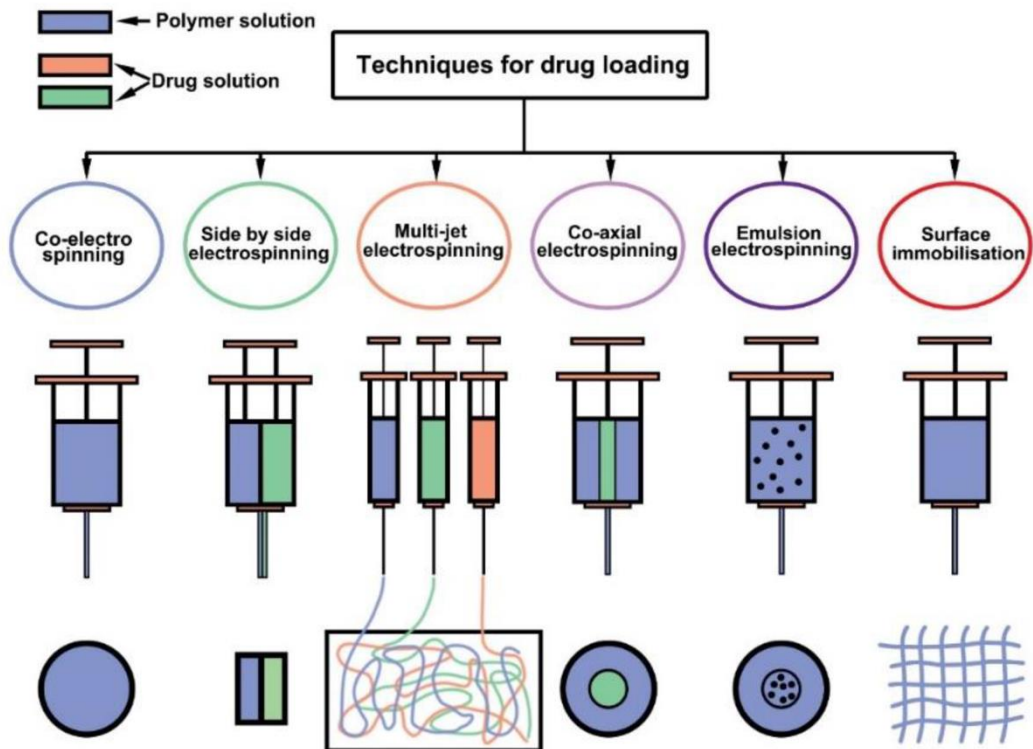


Figure 9 Types of ES [52].

In a study, the change in morphology of particles to nanofibers using low molecular weight amphiphilic copolymers was investigated by using the side-by-side ES technique. Compared to conventional electrospinning with single-component nozzles, side-by-side ES allowed both particles and reversibly cross-linkable fibers to be obtained from the same polymer material [53]. The morphological variation is achieved by selecting suitable process conditions and using specific spinnerets. The side-by-side method offers greater flexibility in the production of particles and fibers from the same polymer, and represents an innovative approach to control the morphology of materials obtained by electrospinning [53].

Another study investigated the application of coaxial electrospinning as a robust technique for the encapsulation of sensitive, water-soluble

biological agents within core-shell nanofibers. This method enables the encapsulation of substances such as growth factors, DNA, and even living organisms in a single step. The technique avoids damage caused by direct contact of the sensitive substances with the organic solvents or harsh emulsification conditions [54]. The outer layer of the nanofibers acts as a barrier and prevents the premature release of the water-soluble molecules present in the core. The study highlighted that the release of the encapsulated active ingredients can be precisely controlled by varying the structure and composition of the nanofibers [54].

3 Materials and Methods

3.1 Synthesis of the PEAs

3.1.1 Synthesis of the bis- α -(L-amino acid)- α , ω -alkylene diesters (BAADs)

Synthesis of bis- α -(L-amino acid)- α , ω -alkylene diesters (BAADs) from 1,6-hexanediol (Hex) (CAS n° 629-11-8, Tokyo Chemical Industry Co., Ltd) and L-phenylalanine (Phe) (CAS n° 63-91-2, Tokyo Chemical Industry Co., Ltd) through Fisher esterification, in toluene (300 mL), at 135°C, during 24h, in presence of p-TSA (CAS n° 6192-52-5, Tokyo Chemical Industry Co., Ltd), as shown in Figure 10. The stoichiometry of the reaction was 2 moles of Phe for 1 mol of Hex, in presence of 2.1 moles of p-TSA. The quantities of each reactant used in the synthesis of the BAAD is presented in Table 1, and the specific machinery used is shown in Figure 11. For purification, the BAAD was submitted to several recrystallizations (Figure 12), using distilled water, and then was dried at 50°C.

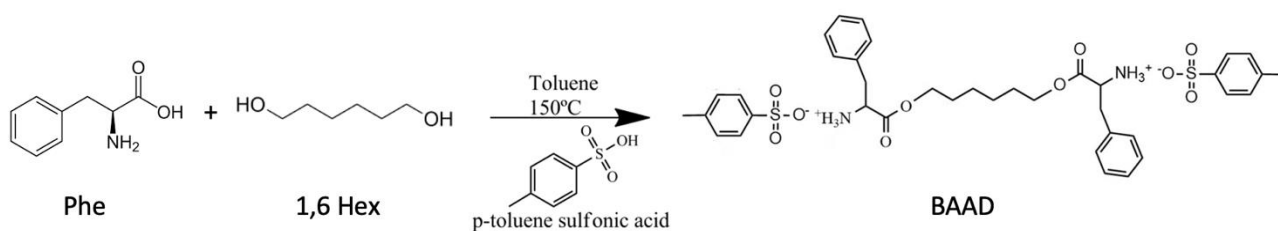


Figure 10 BAAD Synthesis.



Figure 11 Machinery used for the BAAD formation: 500mL round bottomed flask, agitation rod, dean stark, condenser, mineral wool.



Figure 12 BAADs Crystallization.

Table 1 Amount of reactants used in the synthesis of the BAADs.

Reagents	Real Quantity		
	V(mL)	m(g)	n(mol)
Phenylalanine		39.430	0.239
1,6-hexanediol		14.180	0.120
p-TSA		50.050	0.263
Toluene	300		

3.1.2 Synthesis of the PEAs

PEAs derived from Phe were obtained through the reaction of BAAD-Phe with the activated diester of sebacoyl chloride, through a solution polycondensation in dimethylsulfoxide (DMSO), at 70°C, for 24 hours in the presence of triethylamine (Cas n° 121-44-8, Tokyo Chemical Industry Co., Ltd). Figure 13 shows the reaction.

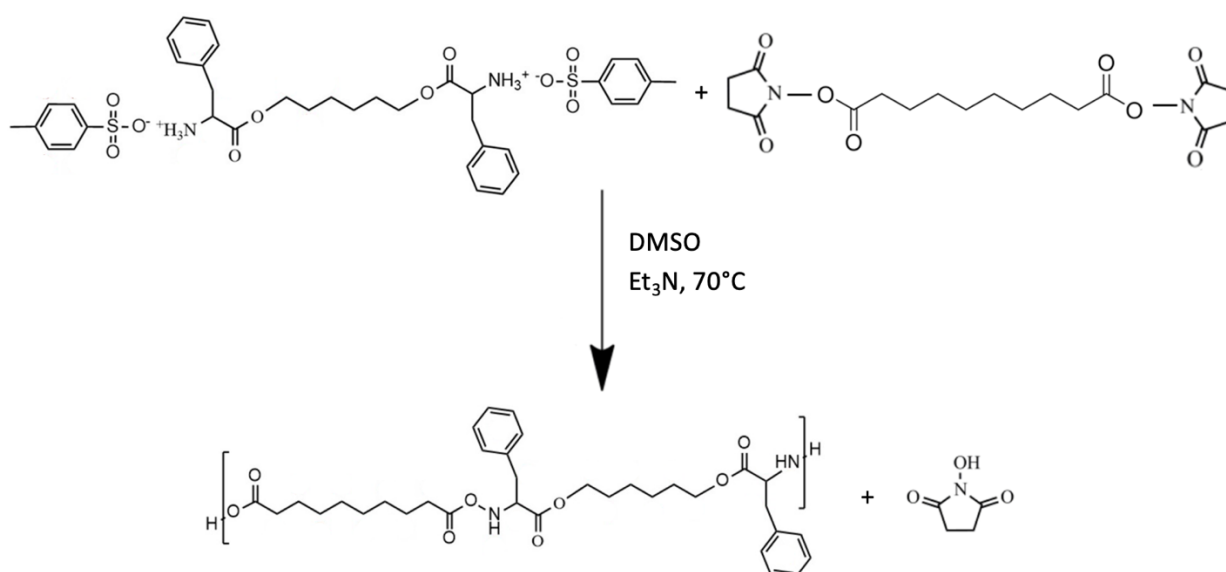


Figure 13 PEAs Synthesis.

Table 2 presents the amount of each reactant used in the synthesis of the PEAs.

Table 2 Amounts of reactants used in the synthesis of PEAs.

PEA	m _{BAAD} (g)	V _{DMSO} (ml)	V _{Et3N} (ml)	m _{activated diester} (g)
ADS_P01	PN_Phe03 – 4.56	10	1.8	2.4
ADS_P02	PN_Phe03 – 4.54	10	1.8	2.37
ADS_P03	ADS_Phe01 – 4.55	10	1.8	2.39
ADS_P04	PN_Phe04 – 4.51	10	1.8	2.38
ADS_P05	ADS_Phe01 – 9.1	20	3.46	4.77
ADS_P06	ADS_Phe01 – 9.09	20	3.46	4.75
ADS_P07	ADS_Phe01 – 9.09	20	3.46	4.78
ADS_P08	ADS_Phe01 – 9.08	20	3.46	4.76
ADS_P09	ADS_Phe01 – 11.27	20	3.16	5.93
ADS_P10	PN_Phe04 – 24.65	20	9.15	13.1

For purification several steps have been implemented. First of all, the reaction product was dissolved in 50 ml of chloroform inside a 1 L cup, followed by the gradual addition of water until the total volume of 1 L was reached. A magnet was inserted into the container, which was subsequently subjected to slow stirring (150 rpm) for 2 days. During this period, the water was replaced three times. Subsequently, after eliminating the water, the PEA dissolved in chloroform was dried by solvent casting.

Then, a further step of purification was carried out, in which the dried PEA was placed in a 100 mL single-throated flask, together with 50 mL of ethyl acetate. The content on the flask was submitted to a temperature of 100°C and a magnetic agitation of 500 rpm. A condenser was connected to the flask to avoid the evaporation of the solvent. After 24

hours, the ethyl acetate was changed, and the waste product was retained for comparison purposes. This procedure was further repeated 2 more times. The PEA was then dried at the end of the process.

3.2 Mats Preparation by Electrospinning-

The solutions needed for the ES process, were prepared by dissolving the PEAs in a mixture of solvents, chloroform and DMSO, with a ratio 90:10 (v/v), respectively. The concentration of PEAs solutions was set at 10% (w/v). To impart specific antimicrobial properties to the membranes, AgSD was introduced into the PEA polymer solution at 0.25% (w/w).

The applied voltage was between 19 and 22kV, distance between the needle tip and collector was established in 20 cm, and solution flow was 2 ml/h. For electrospinning, each solution was loaded into 10 mL syringes with 17G stainless steel flat needles.

The needle was connected to the positive electrode of the high voltage power supply, while the collector, covered with vegetable paper on a surface of 100 cm², was grounded. PEAs nanofibers, generated through electrospinning, were collected on these vegetable paper-based collectors.

The machinery used is shown in Figure 14.



Figure 14 Representation of the ES apparatus used.

3.3 Characterization Techniques

3.3.1 Nuclear Magnetic Resonance (NMR) Spectroscopy

H^1 NMR spectroscopy analysis was performed using a Bruker Avance 400 MHz spectrometer at a temperature of 25 °C. Deuterated DMSO was used as solvent. The peak of DMSO- d_6 (2.50 ppm) was used as reference.

3.3.2 SEC Analysis

Molecular weight distribution was determined using a Size Exclusion Chromatography (SEC) set-up (Viscotek TDAmix) equipped with a differential viscometer (DV) and right-angle laser-light scattering (RALLS, Viscotek) and refractive index (RI) detectors. The column set consists of a 5 μm PLgel pre-column followed by a Viscotek T5000 column and a Viscotek T4000 column. A dual-piston pump was set with a flow rate of 1 mL/min. The eluent (DMF with 0.03% (w/v) LiBr) was previously filtered through a 0.2 μm filter. The system was also equipped with an online degasser. The tests were performed at 60 $^{\circ}\text{C}$ using an Elder CH-150 heater. Before injection (100 μL), the samples were filtered through a polytetrafluoroethylene (PTFE) membrane with a pore size of 0.2 μm . The system was calibrated with narrow poly(methyl methacrylate) (PMMA) standards. Molecular weight ($M_{w,SEC}$) and dispersity ($D = M_w/M_n$) of the synthesized polymers were determined by conventional calibration.

3.3.3 Thermal Analysis

The thermal behavior of the BAADs, PEAs and mats was studied through differential scanning calorimetry (DSC) using a DSC 214 Polyma instrument equipped with an Intracooler 40 cooling unit. The samples were heated at a rate of 5 $^{\circ}\text{C}/\text{min}$ from -95 to 200 $^{\circ}\text{C}$, after having performed a run in which they were heated from 25 $^{\circ}\text{C}$ to 200 $^{\circ}\text{C}$ and subsequently cooled to -95 $^{\circ}\text{C}$.

The thermal stability of the mats obtained via electrospinning was evaluated through thermogravimetric analysis (TGA) using a STA 449

F3 Jupiter instrument. The analysis was conducted in the temperature range of 25 to 1000 °C, in a nitrogen environment, with a heating rate of 10 °C/min.

3.3.4 Scanning Electron Microscopy (SEM)

To explore the morphology of the membranes at the microscopic level, a field emission scanning electron microscopy (FESEM) analysis was conducted with a ZEISS MERLIN Compact/VPCompact, Gemini II instrument.

3.3.5 Contact Angle Analysis

An Attension® optical tensiometer from Biolin Scientific was used to determine the surface contact angle of the membranes. Water drops of 3 µL were used as test liquid. The contact angle was measured after 1s of contact of the droplet with the surface of the membrane and is represented as an average of three measurements.

3.3.6 Tensile tests

The mechanical properties of the PEAs mats were tested using a tensile testing machine (Inspekt solo 2.5, Hegewald & Peschke, Germany). The samples were cut into rectangle shape (10x45 mm). The ends of the samples were mounted on the gripping units of the tensile

testing machine, and an extension rate of 10 mm/min was applied until break.

3.3.7 *In vitro* Cytotoxicity Tests

The potential cytotoxic effect of the electrospun mats was evaluated by a direct method. The electrospun mats were cut in a circular shape to fill the wells of a 96-well cell culture plate (diameter of 0.33 cm) (Orange Scientific NV/SA, B-1420 Braine-l'Alleud, Belgium) and were sterilized with UV light for 30 min, on each side. NIH3T3 fibroblast cells were seeded at a cell density of 1×10^4 cells per well on the surface of each sample and maintained at constant temperature (37 °C) in a humidified air atmosphere containing 5% CO₂, for 1, 3 and 7 days. Cells incubated with a complete medium without a mat were used as controls. Cell viability was determined using the AlamarBlue™ HS Cell Viability assay (ThermoFisher Scientific). After 24 h of incubation, the culture medium was completely removed (to remove unattached cells) and replaced with fresh culture medium supplemented with 10% AlamarBlue™ HS Cell Viability for 3 h at 37 °C. Then, the medium was aspirated and transferred to a new 96-well plate. The absorbance at 570 nm and 600 nm was measured for each sample (with a total of 32 replicates for each sample) using a microplate reader.

3.3.8 Antimicrobial test

Two types of antimicrobial tests were performed. For the Halo-method, bacteria Gram-positive *S. aureus* and Gram-negative *E. coli* were

inoculated into molten agar and covered by the membranes samples once agar got solidified. These plates were incubated for 24 hours at 37°C to measure the zone of inhibition (halo).

For bacteria growth test, the same quantity of bacteria Gram-positive *S. aureus* and Gram-negative *E. coli* were placed to growth, at 37 °C, on medium in which 1 cm² of mat sample was placed. After 24 h, the amount of bacteria was measured through optic density read at 600 nm.

4 Results & Discussion

4.1 BAAD Characterization

The BAAD was characterized in terms of its chemical structure and thermal properties.

4.1.1 ^1H NMR Spectroscopy Analysis of the BAAD

The characterization of the BAAD by ^1H NMR spectroscopy allowed to check if the BAAD was obtained with success.

By observing the spectral peaks in Figure 15, it was possible to identify the different protons associated with the different chemical environments of the molecule and to analyze their mutual interaction.

The spectrum obtained (Figure 15) is in accordance with the anticipated chemical structure. Specifically, the peak (b), between 7 and 7.5 ppm, and the peak (a) between 2 and 2.5 ppm are related with the protons of the aromatic rings and the $-\text{CH}_3$ groups of the p-TSA moieties that are protecting the amino groups. At 8.5 ppm it is possible to find peak (c), ascribed to the protons of the protonated amino groups. Near to 7.3 ppm are the peaks related to the aromatic ring of the Phe (f). At 4.3 ppm, it is possible to find peak (d), which was used as reference for the integration. Between 3.0 and 3.2 ppm are present peak (e) corresponding to the protons of the $-\text{CH}_2$ group of Phe. The peaks (g), (h) and (i) belong to the protons of the Hex aliphatic chain and were found at 4.0, 1.4 and 1.0 ppm, respectively.

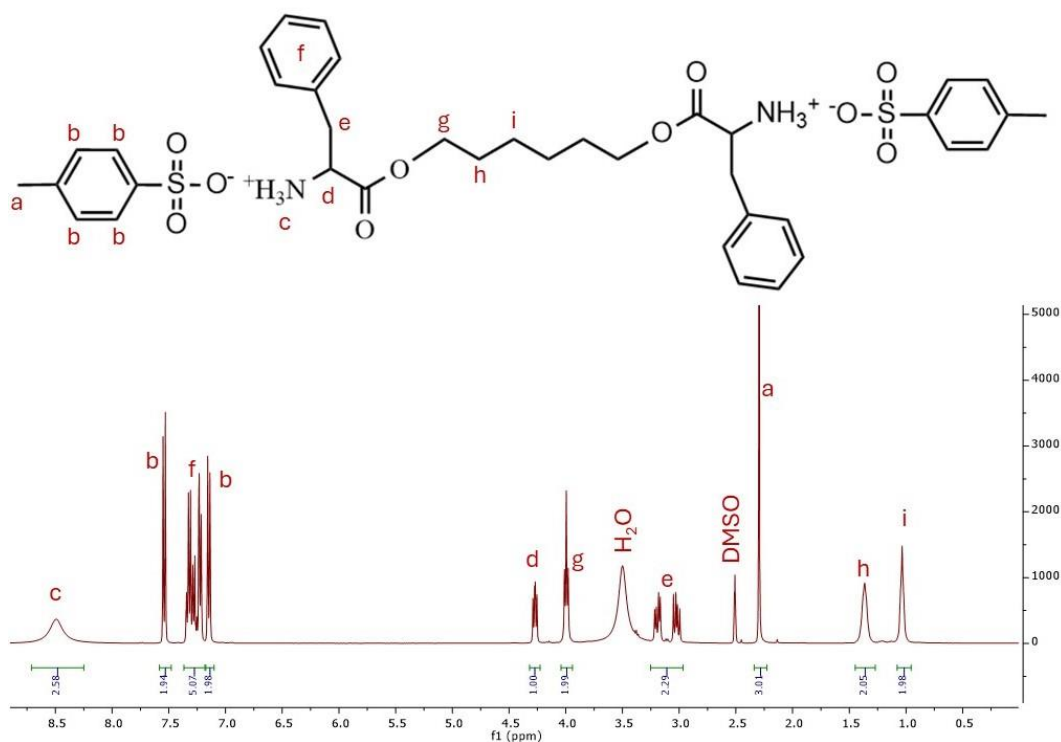


Figure 15 ^1H -NMR Analysis of BAAD.

The yield of the synthesis was 64 %. This yield is considered to be quite good, but could indicate that this synthesis process can be further optimized to increase the yield. This means that there is a gap between the theoretical and actual amounts, which could be due to several factors, including losses during the synthesis process, during the purification steps or other factors that may affect the product yield.

4.1.2 Thermal analysis for BAAD

Figure 16 shows the heat flow curve of the Phe BAAD, where only an event consistent with a glass transition is observed at *ca.* 49 °C. This means that until 200 °C, the highest temperature achieved in the analysis, the BAAD does not melt.

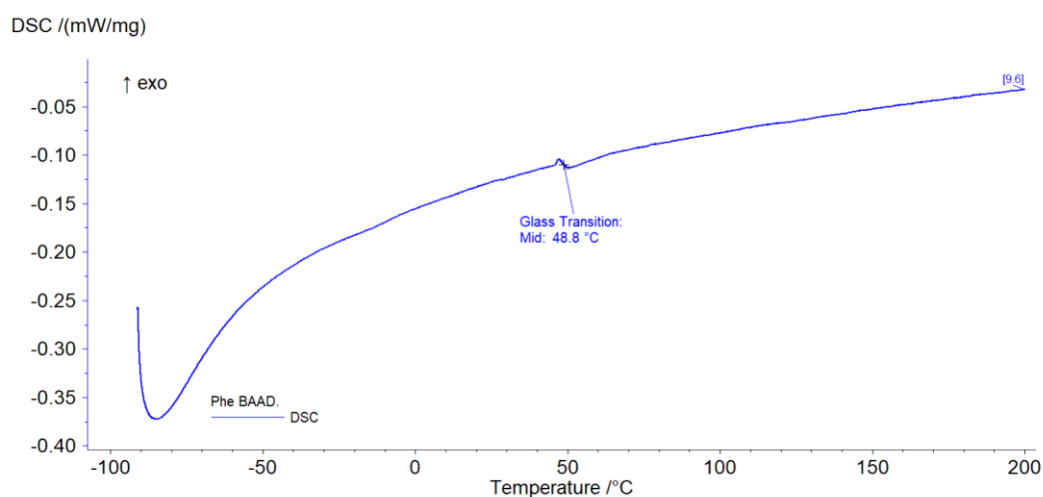


Figure 16 DSC analysis of Phe BAAD. This graphic represents the second heating run of the Phe BAAD since -95°C until 200°C at a heating velocity of 5°C/min.

4.2 Characterization of the PEAs

The PEAs were characterized in terms of their chemical structure, molecular weight distribution and thermal properties.

4.2.1 ¹H NMR Spectroscopy Analysis of the PEAs

Figure 17 presents the ¹H NMR spectrum of ADS_P10, which is representative of the other PEAs obtained.



Figure 17 ^1H NMR spectrum of a PEA-Phe.

As shown, all the protons in the repeating unit of the PEA are present in the spectrum, evidencing that the reaction was successful. The peaks (h), between 7 and 7.5 ppm, are associated with the aromatic rings of the Phe, while at around 8.5 ppm, the peak (c), are ascribed to the protons of the amide linkage. At 4.5 ppm, the peak (f) is found and is attributed to the protons of the -CH group. At *ca.* 3 ppm is found the peak (g), associated with the protons of the CH_2 groups of Phe. The peaks (i), (j) and (k), belonging to the protons of the aliphatic chain of Hex moieties, are located at around 4.0, 1.4 and 1.1 ppm. The peaks (a), (b), (c) and (d) appearing, respectively, at 2, 1.4, 1.2 and 1.1 ppm, correspond to the protons of the aliphatic chain of the activated ester moiety.

4.2.2 Molecular weight distribution of the PEAs

Table 3 presents the values of molecular weight and dispersity of the synthesized PEAs.

Table 3 Molecular weight and dispersity of the PEAs synthesized during the work.

PEA	Yield (%)	M_w (kDa)	\bar{D}
ADS_P01	38	35	1.9
ADS_P02	75	65	1.9
ADS_P03	3	40	1.8
ADS_P04	36	28	1.5
ADS_P05	-	38	2.0
ADS_P06	-	39	2.0
ADS_P07	-	9	1.6
ADS_P08	-	19	1.9
ADS_P09	-	8	1.5
ADS_P10	91	80	1.7

From Table 3, it is possible to observe some discrepancies between the values of molecular weight obtained. In some cases, the BAADs used were from different batches and this could cause some differences in the values of molecular weight. If one of the used BAADs was not properly purified, then this would translate in PEAs of lower molecular weight, due to stoichiometric imbalances. Also, using the exact same BAAD did not translate to PEA with the same molecular weight. It was hypothesized that this could be due to the presence of some moisture in the reactional medium that led to the hydrolysis of the activated diester of the sebacoyl chloride.

Analyzing the yield of all polymerizations, the difference between theoretical and actual mass can be attributed to problems during the polymerizations, losses during the handling or purification processes or to other variations in experimental conditions, namely the presence of moisture in the reaction medium.

4.2.3 Thermal Analysis of the PEAs

From the heat flow curve presented in Figure 18 it is possible to observe that besides the glass transition (at 30.5 °C), no other transition is observed, indicating that the PEA-Phe is amorphous.

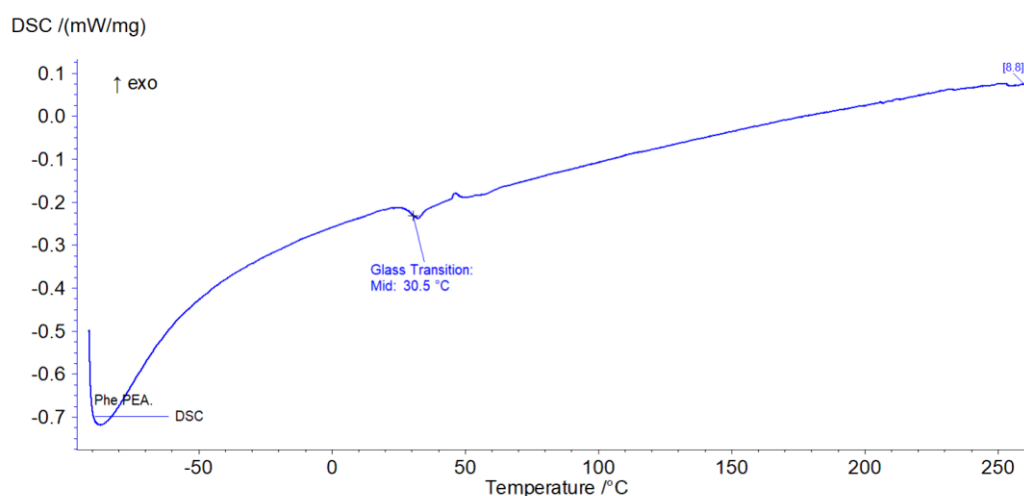


Figure 18 DSC analysis of Phe PEA. This graphic represents the second heating run of the Phe PEA since -95°C until 200°C at a heating rate of 5°C/min.

4.3 ES Membranes Characterization

The parameters for the ES were selected on the basis of preliminary tests and results of an on-going work in the research group where the present work was conducted. Table 4 presents the ES parameters used in the preparation of the different membranes.

Table 4 ES Membranes Parameters.

ES membrane	PEA	m (mg) PEA	m (mg) AgSD	V (ml) CHCl3	V (ml) DMSO	Voltage (kV)	Distance tip - collector (cm)	Flux (ml/h)	Temperature (°C)	Humidity (%)
ADS_ES01	ADS_P02	600	-	5.4	0.6	14.5	20	2	31	30
ADS_ES02	ADS_P02	600	-	5.4	0.6	16.5	20	2	33	20
ADS_ES03	ADS_P02	600	-	5.4	0.6	15.7	20	2	35	20
ADS_ES04	ADS_P02	780	-	6.28	0.78	17	17	2	30	20
ADS_ES05	ADS_P05	600	-	5.4	0.6	-	20	2	-	20
ADS_ES06	ADS_P05	600	-	5.4	0.6	-	20	2	-	20
ADS_ES07	ADS_P05	600	-	5.4	0.6	-	20	2	-	20
ADS_ES08	ADS_P06	600	-	5.4	0.6	17.5	17	2	30	20
ADS_ES09	ADS_P09	600	-	5.4	0.6	17	20	2	28	20
ADS_ES10	ADS_P10	600	-	5.4	0.6	21	20	2	27	20
ADS_ES11	ADS_P10	600	-	5.4	0.6	21.5	20	2	29	20
ADS_ES12	ADS_P10	600	-	5.4	0.6	20.5	20	2	30	20
ADS_ES13	ADS_P10	600	-	5.4	0.6	21.5	20	2	30	20
ADS_ES14	ADS_P10	600	-	5.4	0.6	21.5	20	2	30	20
ADS_ES15	ADS_P10	600	1.5	5.4	0.6	19.5	20	2	31	20
ADS_ES16	ADS_P10	600	1.5	5.4	0.6	19.5	20	2	30	20
ADS_ES17	ADS_P10	600	1.5	5.4	0.6	20.5	20	2	32	20
ADS_ES18	ADS_P10	600	1.5	5.4	0.6	20.5	20	2	33	20
ADS_ES19	ADS_P10	600	1.5	5.4	0.6	21	20	2	32	20
ADS_ES20	ADS_P10	600	1.5	5.4	0.6	20.5	20	2	31	20
ADS_ES21	ADS_P10	600	-	5.4	0.6	21.5	20	2	31	20

The membranes subjected to characterization were those based on the PEA ADS_P10. This choice was driven by the fact that this particular PEA yielded the highest M_w , a crucial factor for producing nanofibrous mats with good quality. For the obtainment of high-quality fibers, it is necessary to have PEAs with molecular weight higher than 60 kDa.

In fact, the use of PEAs with a molecular weight lower than 60 kDa (attempts ADS_ES05, ADS_ES06, ADS_ES07 and ADS_ES09), did not allowed to obtain any kind of membrane.

4.3.1 Morphology of the membranes

The SEM analysis of the membranes revealed the presence of beads or thickenings in the fibers, as shown in Figure 19. Despite the presence of these beads, the SEM images show a significant similarity between the membranes with and without antibacterial agent, suggesting that the presence of this agent did not lead to significant changes in the morphological properties of the membranes.

The defects observed in the membranes might be due to the specific parameters used during the ES process. It is hypothesized that these thickenings can be reduced or avoided by adjusting some key parameters, such as increasing the voltage or reducing the flow. Increase in the temperature could be an additional factor to consider to solve this problem.

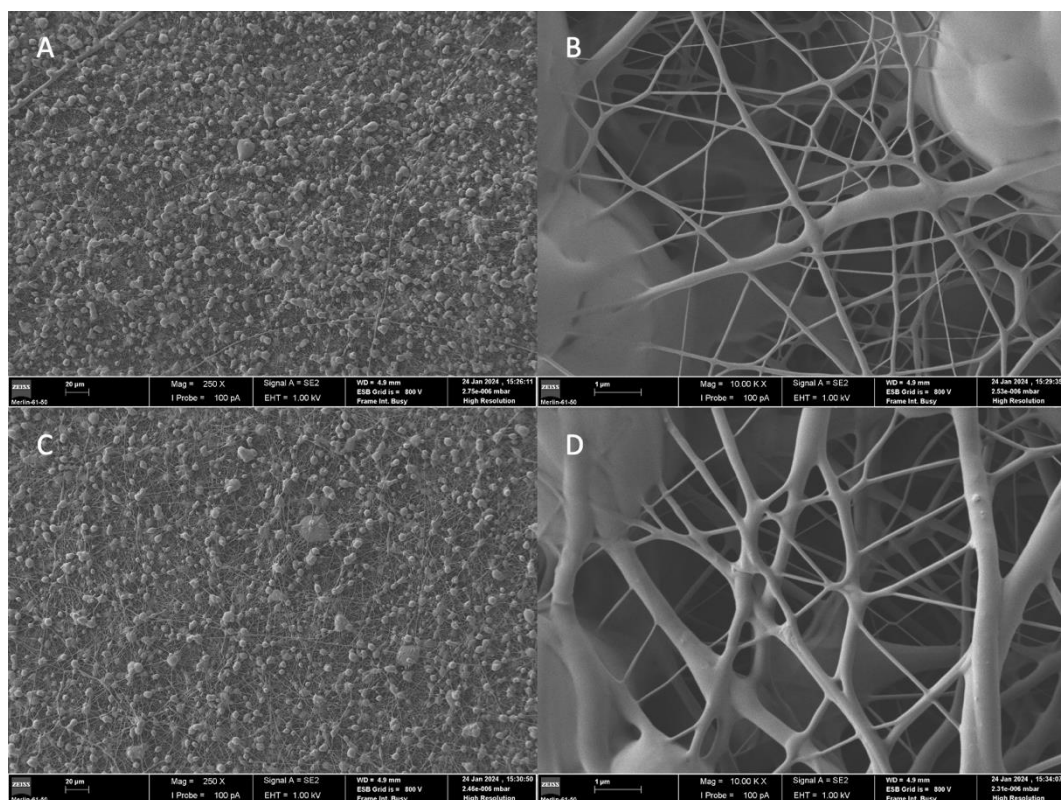


Figure 19 (A) SEM image of membrane ADS_ES13 (no antimicrobial agent) with amplification of 250x. (B) SEM image of membrane ADS_ES13 with amplification of 10.000x. (C) SEM image of membrane ADS_ES15 (with antimicrobial agent) with amplification of 250x. (D) SEM image of membrane ADS_ES15 with amplification of 10.000x.

4.3.2 ^1H NMR spectroscopy analysis to the membrane

The ^1H NMR analyses was also performed to the membranes. As shown in Figure 20, the spectrum obtained is almost identical to the one of the PEAs, as expected. This result confirms that the chemical structure of PEA was not changed during the ES process. In addition, the PEA was dissolved in chloroform and DMSO before the ES process, and no chloroform and DMSO were detected when the membrane was analyzed, confirming that both solvents evaporated during the ES process, as was supposed to occur.

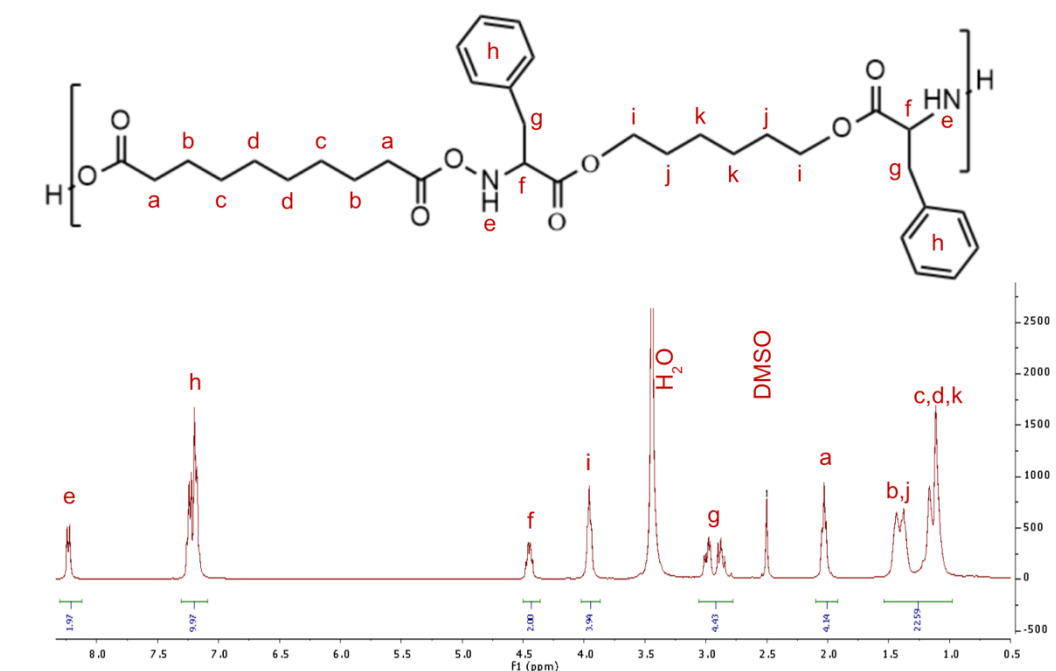


Figure 20 Exemplificative ^1H NMR spectrum of the membrane.

The membrane containing AgSD was also subjected to NMR analysis, to try to demonstrate the effective incorporation of the active compound. Unfortunately, it was not possible to confirm the presence of AgSD using this technique.


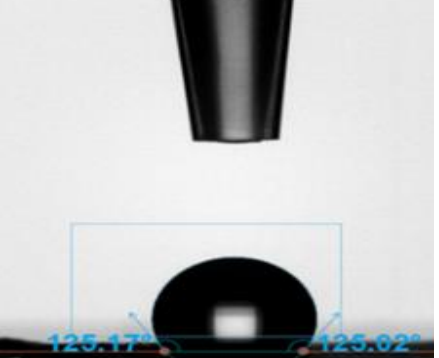
4.3.3 Contact Angle

Contact angle analysis was conducted on membranes both with and without AgSD.

Very similar values were obtained between membranes with and without AgSD (Table 5). Both types of membranes show a very pronounced hydrophobic behavior, with the contact angles indicating a highly hydrophobic surface. The hydrophobicity of the membrane can be attributed to the both hydrophobic nature of the Phe and the long aliphatic chain of Hex used in PEA synthesis.

Typical hydrophilic surfaces have contact angle values that range from less than 10° (superhydrophilic) to 90°(hydrophilic), while values above 150°indicate a superhydrophobic surface.

Table 5 Contact Angle test results.

Samples	Contact Angle (°)	
Membrane with AgSD	127.2±4.7	
Membrane without AgSD	123.1±8.4	

4.3.4 Thermal Analysis for ES membranes

Figure 21 shows the heat flow curves of the electrospun membranes with and without AgSD. The heat flow curve shows that both membranes exhibit similar thermal behavior, with similar T_g values, and an amorphous nature.

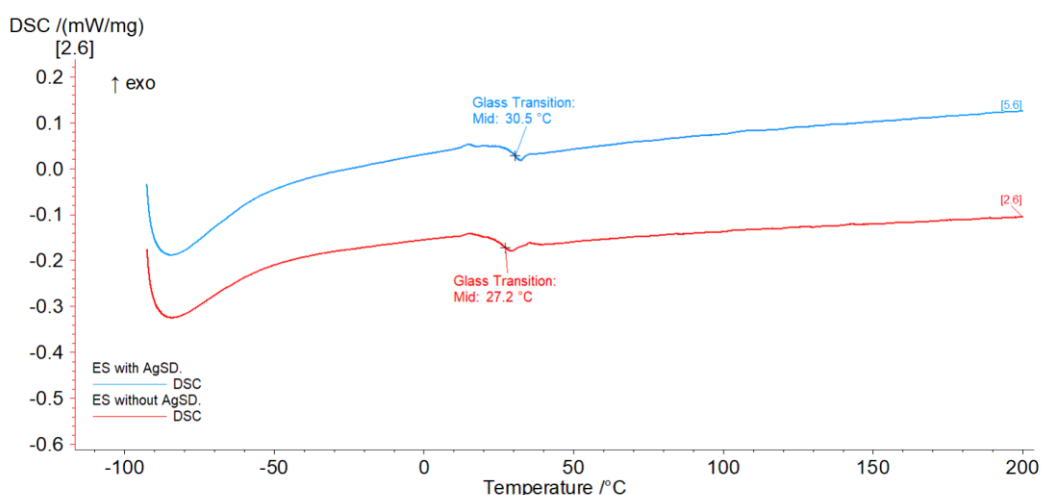


Figure 21 DSC analyses of ES membranes with and without AgSD. ES14 was used as representative of the membranes without AgSD and the ES20 was used as representative of the membranes with AgSD. This graphic represents the second heating run of each membrane, since -95°C until 200°C at a heating velocity of 5°C/min.

Regarding the TGA analysis, Figure 22 shows that both membranes present similar thermal stability, losing 5% of their initial weight at very similar temperatures (341°C and 345°C for the membranes without and with AgSD, respectively).

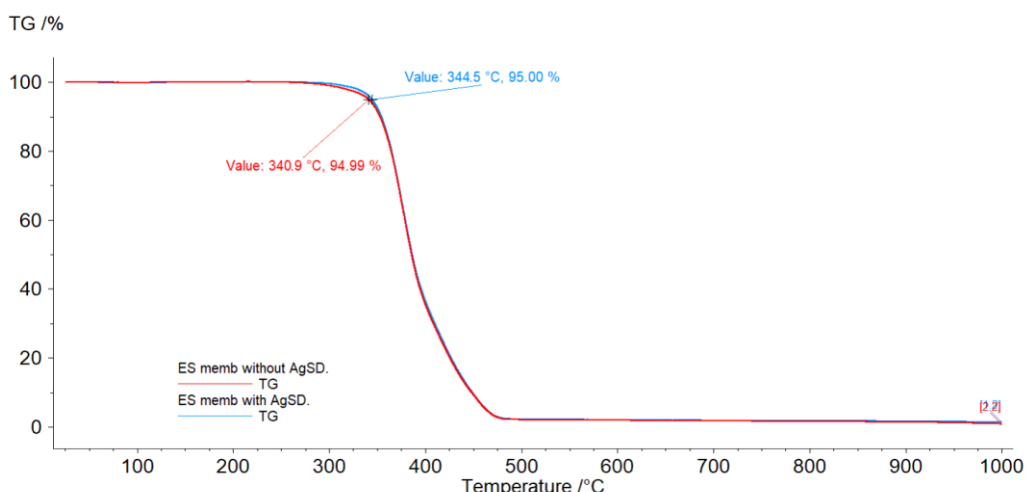


Figure 22 TGA analyses of ES membranes with and without AgSD. ES14 was used as representative of the membranes without AgSD and the ES20 was used as representative of the membranes with AgSD. This graphic represents the heating run of each membrane, since 25°C until 1000°C at a heating velocity of 10°C/min.

4.3.5 Tensile Tests

The mechanical properties of the membranes were analyzed using the tensile test, that evaluates the resistance and deformability of materials. For each membrane, 3 to 5 samples were analyzed, and from the results various parameters were extrapolated. The parameters that have been analyzed were:

- E (Young's Modulus): measures the stiffness of the material and its ability to deform under load.
- σ_{\max} (Maximum Stress): represents the maximum stress the material can withstand before breaking.
- Elongation (%): indicates the percentage of maximum elongation before breaking.
- F_{\max} (Maximum Force): indicates the maximum tensile force that the sample can withstand before it breaks.

These parameters provide information on the mechanical performance of the membranes and provide important information for biomedical and engineering applications. The variability between samples was carefully considered when interpreting the results. For each membrane, the average and standard deviation of these parameters were calculated for all samples tested; the results are shown in Table 6. The aim is to evaluate the variability within each membrane type and to compare the differences between membranes with and without the antibacterial agent.

Table 6 Statistic Analysis of the membranes.

Samples		E[MPa]	σ Max[MPa]	Elongation[%]	Fmax[N]
Membrane with AgSD	Average	0.03	1.3	169.54	1.28
	St. Dev.	0.01	0.33	54.96	0.33
Membrane without AgSD	Average	0.02	0.89	116.15	0.88
	St. Dev.	0.01	0.23	30.38	0.23

When analyzing for the presence or absence of AgSD the results obtained from the tensile tests show that the membranes containing AgSD have higher values for the four parameters analyzed (E, σ Max, elongation, Fmax) than the membranes without AgSD (Figure 23). However, there are some considerations to be made. The lack of a highly accurate measurement of membrane thickness can be a factor responsible for the differences observed.

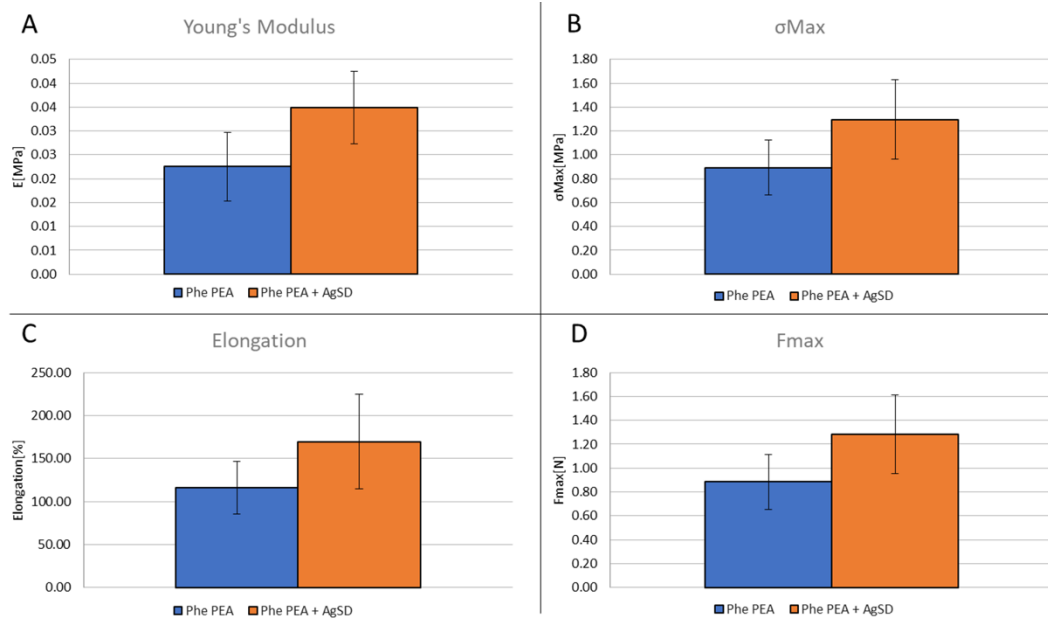


Figure 23 Tensile analyses comparison between membranes with or without AgSD. A) Young's modulus analysis; B) Maximum Stress Analysis; C) Elongation Analysis; D) Maximum Force Analysis.

4.3.6 *In vitro* Cytotoxicity Tests

To confirm that the membranes are suitable for use as WD, an *in vitro* cytotoxicity analysis was performed on fibroblasts. The cells were brought into contact with membranes with and without AgSD to whether there were significant differences. The analyzes were carried out over a period of seven days to determine whether the membranes had any toxic effects within this period.

Figure 24 shows that all membranes show no cytotoxicity during the time for the fibroblasts. On day 1, the viabilities were very similar between the membranes and the control. On day 3, the membranes without AgSD showed similar viability to day 1. Although the viability of the membranes with AgSD decreased slightly on day 3, the percentage of living cells were close to 90%, indicating that these membranes are still viable for the envisaged application. On day 7, both

membranes again showed similar results close to 90% viability. These results suggest that the membranes have no toxic effects on the fibroblasts in the first seven days, and it is expected that this viability could be achieved in further days of incubation.

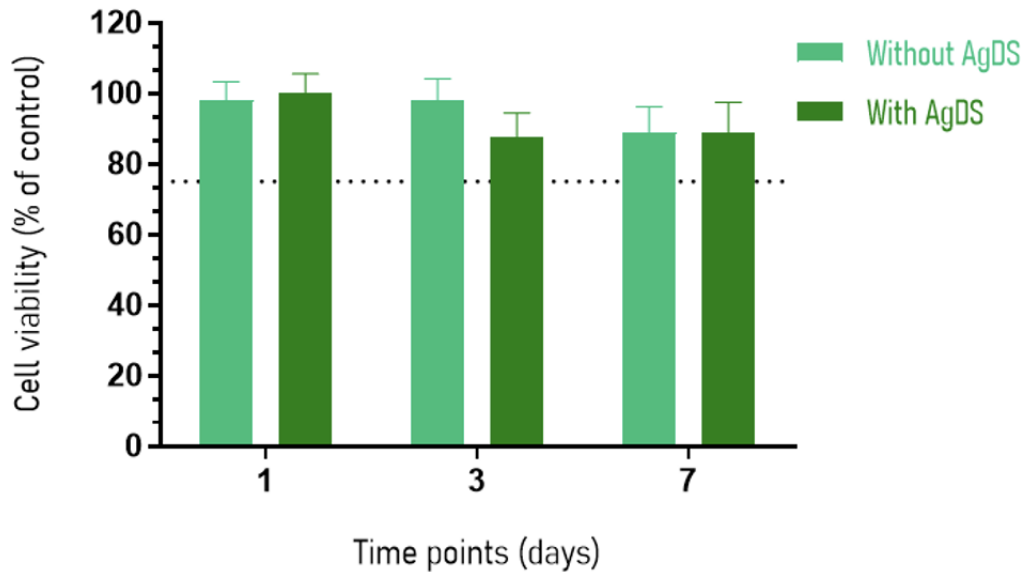


Figure 24 Cytotoxicity analysis of the membranes with and without AgSD on fibroblasts at 1, 3 and 7 days of incubation.

4.3.7 Antimicrobial Tests

In addition to the *in vitro* cytotoxicity tests, *in vitro* antibacterial tests were also carried out. The results of the antimicrobial tests provide important information on the effectiveness of the membranes against Gram-positive *S. aureus* and Gram-negative *E. coli* bacteria.

In the halo method, the antibacterial activity is evaluated based on the "zone of inhibition" around the treated sample. Figure 25, which shows the results for the membranes ADS_ES15 (with AgSD) and ADS_ES13 (without AgSD), shows no activity against either type of bacteria. This

indicates that the membranes do not diffuse the AgSD present on them under the specific experimental conditions and therefore have no effect on inhibiting bacterial growth.

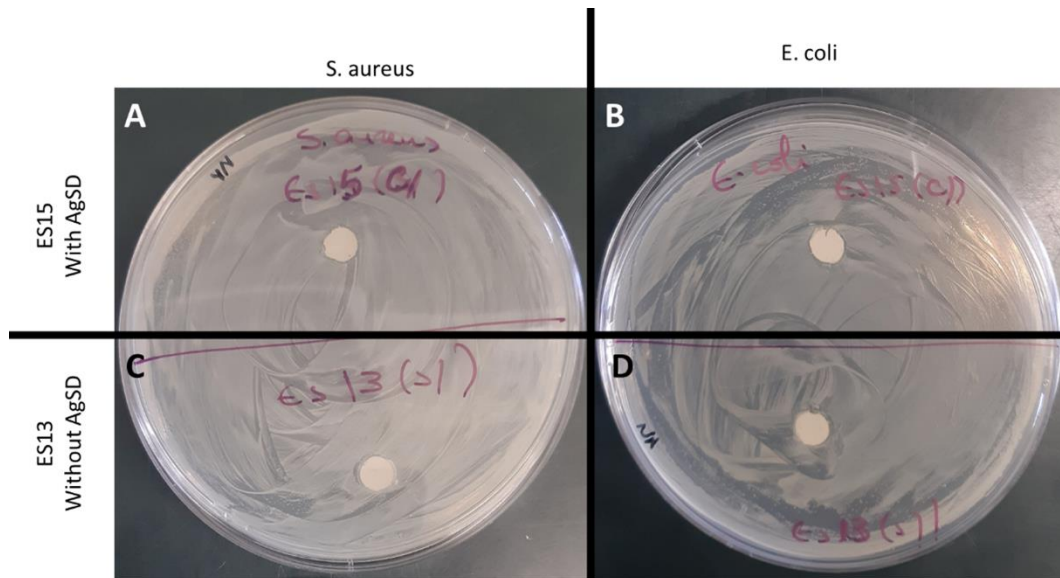


Figure 25 Images of Halo test for the membranes ADS_ES13(without AgSD) and ADS_ES15(with AgSD). (A) ES_15 in presence of bacteria Gram-positive *S. aureus*; (B) ES_15 in presence of bacteria Gram-negative *E. coli*; (C) ES_13 in presence of bacteria Gram-positive *S. aureus*; (D) ES_15 in presence of bacteria Gram-negative *E. coli*.

For the bacterial growth test, where a known number of bacteria were grown in the presence of the membrane, data analysis revealed no antimicrobial activity. The quantity of bacteria measured by reading the optical absorbance at 600 nm does not show statistically significant differences between the membranes with and without the antibacterial agent. The membranes with AgSD presented a viability near 100% for both Gram-positive *S. aureus* and Gram-negative *E. coli* bacteria.

The outcome from the antibacterial tests can be a consequence of the strong hydrophobicity of the membranes, highlighted by the water contact angle value, could be one of the reasons for the limited diffusion

of AgSD. Water resistance may have influenced the release of the active ingredient, thus reducing its ability to counteract bacterial growth.

Therefore, results underline the fact that the membranes do not exhibit effective antimicrobial activity against the bacteria considered under the specific conditions of the tests performed.

5 Conclusions

The synthesis of the BAAD was successfully conducted, as confirmed by the ^1H NMR analysis which revealed the desired chemical structure. The yield of the synthesis process was ca. 64%, indicating reasonable success but suggesting room for further optimization to increase the yield.

The PEAs were also obtained with success as revealed by ^1H NMR spectroscopy and SEC. From the PEA with a molecular weight of ca. 80 kDa it was possible to prepare membranes by ES process. Despite some morphological irregularities in the SEM images, the membranes showed well-defined fibers. Tensile tests indicated improved strength and deformability in membranes with the AgSD antibacterial agent, although more in-depth analysis considering the variation in thickness is required. In vitro cytotoxic tests confirmed the safety of the membranes for WD applications, but the antimicrobial studies revealed no activity against *S. aureus* and *E. coli*.

Unfortunately, the results of the tests with AgSD did not meet the original expectations, which underlines the unpredictability and complexity of scientific research. Despite the successful synthesis of BAAD and the efficient production of PEAs and membranes by electrospinning, analysis of the AgSD-containing membranes revealed that they did not exhibit significant antimicrobial activity.

6 Future Developments

The future developments of this research offer a promising perspective, with a on testing of a new antibacterial agent, curcumin, which appears to have a greater affinity for membranes. This study phase aims to fully explore the potential of curcumin as an antibacterial agent in WD. Curcumin, known for its antimicrobial and anti-inflammatory properties, approves to be a potential alternative to the previously tested antibacterial agent, opening up new research horizons. Evaluation of the effectiveness of curcumin will be essential to understand its impact on bacterial resistance. In parallel, optimizing the conditions of curcumin incorporation into the ES process will be a key point. Ensuring uniform distribution of this compound during membrane production will be crucial to maximize its antibacterial properties. Moreover, future developments will also focus on further refining the parameters associated with the ES process to improve the morphological and functional characteristics of the membranes, thus contributing to the production of more advanced and effective WD.

In summary, the exploration of curcumin as a new antibacterial agent, optimization of PEAs synthesis and the optimization of membrane production processes represent interesting perspectives for the enhancement of WD, with the aim of offering more effective solutions in the treatment of wounds.

List of Figures

Figure 1 Schematic comparison of chronic and acute wound microenvironment [3].	14
Figure 2 The features of the ideal WD [1].	17
Figure 3 Synthesis of PEAs containing α -amino acids from a thermal polycondensation of a diol and a diamide–diester. R and R ₂ , alkyl chain of variable length; R ₁ , α -amino acid side chain [32].	25
Figure 4 Solution polycondensation method for the preparation of α -amino acid-based PEAs. R and R ₂ are aromatic or aliphatic chains of variable length and R ₁ is the α -amino acid side chain [32].	26
Figure 5 Synthesis of α -amino acid PEAs by interfacial polycondensation.	27
Figure 6 The solvent-casting process [41].	29
Figure 7 Schematic exemplification of the conventional ES process [45].	31
Figure 8 High-speed photographs showing the disintegration of a levitated droplet of ethylene glycol charged to the Rayleigh limit for the ejection of two jets [46].	32
Figure 9 Types of ES [51].	35
Figure 10 BAAD Synthesis.	37
Figure 11 Machinery used for the BAAD formation: 500mL round bottomed flask, agitation rod, dean stark, condenser, mineral wool.	38
Figure 12 BAADs Crystallization.	38
Figure 13 PEAs Synthesis.	39
Figure 14 Schematic representation of the electrospinning apparatus, with the collector positioned in the vertical position, from [53].	42
Figure 15 H ¹ -NMR Analysis of BAAD.	48
Figure 16 DSC analysis of Phe BAAD. This graphic represents the second heating run of the Phe BAAD since -95°C until 200°C at a heating velocity of 5°C/min.	49
Figure 17 ¹ H NMR spectrum of a PEA-Phe.	50
Figure 18 DSC analysis of Phe PEA. This graphic represents the second heating run of the Phe PEA since -95°C until 200°C at a heating rate of 5°C/min.	52
Figure 19 (A) SEM image of membrane ADS_ES13 (no antimicrobial agent) with amplification of 250x. (B) SEM image of membrane ADS_ES13 with amplification of 10.000x. (C) SEM image of membrane ADS_ES15 (with antimicrobial agent) with amplification of 250x. (D) SEM image of membrane ADS_ES15 with amplification of 10.000x.	56
Figure 20 Exemplificative ¹ H NMR spectrum of the membrane.	57

Figure 21 DSC analyses of ES membranes with and without AgSD. ES14 was used as representative of the membranes without AgSD and the ES20 was used as representative of the membranes with AgSD. This graphic represents the second heating run of each membrane, since -95°C until 200°C at a heating velocity of 5°C/min. 59

Figure 22 TGA analyses of ES membranes with and without AgSD. ES14 was used as representative of the membranes without AgSD and the ES20 was used as representative of the membranes with AgSD. This graphic represents the heating run of each membrane, since 25°C until 1000°C at a heating velocity of 10°C/min. 59

Figure 23 Tensile analyses comparison between membranes with or without AgSD. A) Young's modulus analysis; B) Maximum Stress Analysis; C) Elongation Analysis; D) Maximum Force Analysis. 62

Figure 24 Cytotoxicity analysis of the membranes with and without AgSD on fibroblasts at 1, 3 and 7 days of incubation. 63

Figure 25 Images of Halo test for the membranes ADS_ES13(without AgSD) and ADS_ES15(with AgSD). (A) ES_15 in presence of bacteria Gram-positive S.aureus; (B) ES_15 in presence of bacteria Gram-negative E.coli; (C) ES_13 in presence of bacteria Gram-positive S.aureus; (D) ES_15 in presence of bacteria Gram-negative E.coli. 64

List of Tables

Table 1 Amount of reactants used in the synthesis of the BAADs. ...	39
Table 2 Amounts of reactants used in the synthesis of PEAs.	40
Table 3 Molecular weight and dispersity of the PEAs synthesized during the work.	51
Table 4 ES Membranes Parameters.	54
Table 5 Contact Angle test results.	58
Table 6 Statistic Analysis of the membranes.	61

Bibliography

- [1] E. A. Kamoun, E.-R. S. Kenawy, and X. Chen, “A review on polymeric hydrogel membranes for wound dressing applications: PVA-based hydrogel dressings,” *J. Adv. Res.*, vol. 8, no. 3, pp. 217–233, May 2017, doi: 10.1016/j.jare.2017.01.005.
- [2] V. Vivcharenko and A. Przekora, “Modifications of Wound Dressings with Bioactive Agents to Achieve Improved Pro-Healing Properties,” *Appl. Sci.*, vol. 11, no. 9, Art. no. 9, Jan. 2021, doi: 10.3390/app11094114.
- [3] D. Queen, H. Orsted, H. Sanada, and G. Sussman, “A dressing history,” *Int. Wound J.*, vol. 1, no. 1, pp. 59–77, Apr. 2004, doi: 10.1111/j.1742-4801.2004.0009.x.
- [4] A. A. Rogers, R. S. Walmsley, M. G. Rippon, and P. G. Bowler, “Adsorption of serum-derived proteins by primary dressings: implications for dressing adhesion to wounds,” *J. Wound Care*, vol. 8, no. 8, pp. 403–406, Sep. 1999, doi: 10.12968/jowc.1999.8.8.25910.
- [5] O. Alvarez, “Moist environment for healing: matching the dressing to the wound,” *Ostomy. Wound Manage.*, vol. 21, pp. 64–83, 1988.
- [6] A. J. Nemeth, W. H. Eaglstein, J. R. Taylor, L. J. Peerson, and V. Falanga, “Faster healing and less pain in skin biopsy sites treated with an occlusive dressing,” *Arch. Dermatol.*, vol. 127, no. 11, pp. 1679–1683, Nov. 1991.
- [7] *Advances in Skin & Wound Care*. Elizabeth A. Ayello, PhD, MS, RN, CWON, FAAN and R. Gary Sibbald, MD, MEd, JM.
- [8] J. B. Shah, “The History of Wound Care,” *J. Am. Coll. Certif. Wound Spec.*, vol. 3, no. 3, pp. 65–66, Sep. 2011, doi: 10.1016/j.jcws.2012.04.002.
- [9] R. J. Cornell and L. G. Donaruma, “2-Methacryloxytropones. Intermediates for the Synthesis of Biologically Active Polymers,” *J. Med. Chem.*, vol. 8, no. 3, pp. 388–390, May 1965, doi: 10.1021/jm00327a025.
- [10] M. Parcheta and M. Sobiesiak, “Preparation and Functionalization of Polymers with Antibacterial Properties—Review of the Recent Developments,” *Materials*, vol. 16, no. 12, p. 4411, Jun. 2023, doi: 10.3390/ma16124411.
- [11] J. Cai and R. Liu, “Introduction to Antibacterial Biomaterials,” *Biomater. Sci.*, vol. 8, no. 24, pp. 6812–6813, 2020, doi: 10.1039/D0BM90100H.
- [12] C. Muñoz-Núñez, M. Fernández-García, and A. Muñoz-Bonilla,

- “Chitin Nanocrystals: Environmentally Friendly Materials for the Development of Bioactive Films,” *Coatings*, vol. 12, no. 2, p. 144, Jan. 2022, doi: 10.3390/coatings12020144.
- [13] J. Li *et al.*, “Chitosan Natural Polymer Material for Improving Antibacterial Properties of Textiles,” *ACS Appl. Bio Mater.*, vol. 4, no. 5, pp. 4014–4038, May 2021, doi: 10.1021/acsabm.1c00078.
- [14] E. A. El-Hefian, M. M. Nasef, and A. H. Yahaya, “Chitosan-Based Polymer Blends: Current Status and Applications”.
- [15] K. Jung, N. Corrigan, E. H. H. Wong, and C. Boyer, “Bioactive Synthetic Polymers,” *Adv. Mater.*, vol. 34, no. 2, p. 2105063, Jan. 2022, doi: 10.1002/adma.202105063.
- [16] G. J. Gabriel *et al.*, “Comparison of Facially Amphiphilic versus Segregated Monomers in the Design of Antibacterial Copolymers,” *Chem. – Eur. J.*, vol. 15, no. 2, pp. 433–439, Jan. 2009, doi: 10.1002/chem.200801233.
- [17] L. Tamayo, H. Palza, J. Bejarano, and P. A. Zapata, “Polymer Composites With Metal Nanoparticles,” in *Polymer Composites with Functionalized Nanoparticles*, Elsevier, 2019, pp. 249–286. doi: 10.1016/B978-0-12-814064-2.00008-1.
- [18] M. Alavi and A. Nokhodchi, “An overview on antimicrobial and wound healing properties of ZnO nanobiofilms, hydrogels, and bionanocomposites based on cellulose, chitosan, and alginate polymers,” *Carbohydr. Polym.*, vol. 227, p. 115349, Jan. 2020, doi: 10.1016/j.carbpol.2019.115349.
- [19] M. I. Rahmah, R. S. Sabry, and W. J. Aziz, “Preparation and Antibacterial Activity of Superhydrophobic Modified ZnO/PVC Nanocomposite,” *J. Bionic Eng.*, vol. 19, no. 1, pp. 139–154, Jan. 2022, doi: 10.1007/s42235-021-00106-8.
- [20] Z. Wang, M. R. Bockstaller, and K. Matyjaszewski, “Synthesis and Applications of ZnO/Polymer Nanohybrids,” *ACS Mater. Lett.*, vol. 3, no. 5, pp. 599–621, May 2021, doi: 10.1021/acsmaterialslett.1c00145.
- [21] E. Calce, E. Mignogna, V. Bugatti, M. Galdiero, V. Vittoria, and S. De Luca, “Pectin functionalized with natural fatty acids as antimicrobial agent,” *Int. J. Biol. Macromol.*, vol. 68, pp. 28–32, Jul. 2014, doi: 10.1016/j.ijbiomac.2014.04.011.
- [22] G. Casillas-Vargas *et al.*, “Antibacterial fatty acids: An update of possible mechanisms of action and implications in the development of the next-generation of antibacterial agents,” *Prog. Lipid Res.*, vol. 82, p. 101093, Apr. 2021, doi: 10.1016/j.plipres.2021.101093.
- [23] B. J. Privett *et al.*, “Synergy of Nitric Oxide and Silver Sulfadiazine against Gram-Negative, Gram-Positive, and Antibiotic-Resistant Pathogens,” *Mol. Pharm.*, vol. 7, no. 6, pp. 2289–2296, Dec.

- 2010, doi: 10.1021/mp100248e.
- [24] C. L. Fox and S. M. Modak, "Mechanism of Silver Sulfadiazine Action on Burn Wound Infections," *Antimicrob. Agents Chemother.*, vol. 5, no. 6, pp. 582–588, Jun. 1974, doi: 10.1128/AAC.5.6.582.
- [25] H. S. Rosenkranz and H. S. Carr, "Silver Sulfadiazine: Effect on the Growth and Metabolism of Bacteria," *Antimicrob. Agents Chemother.*, vol. 2, no. 5, pp. 367–372, Nov. 1972, doi: 10.1128/AAC.2.5.367.
- [26] P. Li, L. Wu, B. Li, Y. Zhao, and P. Qu, "Highly water-dispersible silver sulfadiazine decorated with polyvinyl pyrrolidone and its antibacterial activities," *Mater. Sci. Eng. C*, vol. 60, pp. 54–59, Mar. 2016, doi: 10.1016/j.msec.2015.11.021.
- [27] D. Akbik, M. Ghadiri, W. Chrzanowski, and R. Rohanizadeh, "Curcumin as a wound healing agent," *Life Sci.*, vol. 116, no. 1, pp. 1–7, Oct. 2014, doi: 10.1016/j.lfs.2014.08.016.
- [28] A. Rodriguez-Galan, L. Franco, and J. Puiggali, "Degradable Poly(ester amide)s for Biomedical Applications," *Polymers*, vol. 3, no. 1, pp. 65–99, Dec. 2010, doi: 10.3390/polym3010065.
- [29] U. Edlund and A.-C. Albertsson, "Polyesters based on diacid monomers," *Adv. Drug Deliv. Rev.*, vol. 55, no. 4, pp. 585–609, Apr. 2003, doi: 10.1016/S0169-409X(03)00036-X.
- [30] H. Sun, F. Meng, A. A. Dias, M. Hendriks, J. Feijen, and Z. Zhong, " α -Amino Acid Containing Degradable Polymers as Functional Biomaterials: Rational Design, Synthetic Pathway, and Biomedical Applications," *Biomacromolecules*, vol. 12, no. 6, pp. 1937–1955, Jun. 2011, doi: 10.1021/bm200043u.
- [31] A. C. Fonseca, M. H. Gil, and P. N. Simões, "Biodegradable poly(ester amide)s – A remarkable opportunity for the biomedical area: Review on the synthesis, characterization and applications," *Prog. Polym. Sci.*, vol. 39, no. 7, pp. 1291–1311, Jul. 2014, doi: 10.1016/j.progpolymsci.2013.11.007.
- [32] A. Díaz, R. Katsarava, and J. Puiggali, "Synthesis, properties and applications of biodegradable polymers derived from diols and dicarboxylic acids: from polyesters to poly(ester amide)s," *Int. J. Mol. Sci.*, vol. 15, no. 5, pp. 7064–7123, Apr. 2014, doi: 10.3390/ijms15057064.
- [33] L. Asín, E. Armelin, J. Montané, A. Rodríguez-Galán, and J. Puiggali, "Sequential poly(ester amide)s based on glycine, diols, and dicarboxylic acids: Thermal polyesterification versus interfacial polyamidation. Characterization of polymers containing stiff units," *J. Polym. Sci. Part Polym. Chem.*, vol. 39, no. 24, pp. 4283–4293, Dec. 2001, doi: 10.1002/pola.10082.
- [34] J. Montané, E. Armelin, L. Asín, A. Rodríguez-Galán, and J.

- Puiggali, “Comparative degradation data of polyesters and related poly(ester amide)s derived from 1,4-butanediol, sebacic acid, and α -amino acids,” *J. Appl. Polym. Sci.*, vol. 85, no. 9, pp. 1815–1824, Aug. 2002, doi: 10.1002/app.10379.
- [35] A. Rodríguez-Galán, L. Franco, and J. Puiggali, “BIODEGRADABLE POLY (ESTER AMIDE) S: SYNTHESIS AND APPLICATIONS”.
- [36] W. Khan, S. Muthupandian, S. Farah, N. Kumar, and A. J. Domb, “Biodegradable Polymers Derived From Amino Acids,” *Macromol. Biosci.*, vol. 11, no. 12, pp. 1625–1636, Dec. 2011, doi: 10.1002/mabi.201100324.
- [37] P. Ranganathan, C.-W. Chen, S.-P. Rwei, Y.-H. Lee, and S. K. Ramaraj, “Methods of synthesis, characterization and biomedical applications of biodegradable poly(ester amide)s- A review,” *Polym. Degrad. Stab.*, vol. 181, p. 109323, Nov. 2020, doi: 10.1016/j.polymdegradstab.2020.109323.
- [38] B. H. Al-Tayyem and B. A. Sweileh, “Synthesis, characterization and hydrolytic degradation of novel biodegradable poly(ester amide)s derived from Isosorbide and α -amino acids,” *J. Polym. Res.*, vol. 27, no. 5, p. 120, May 2020, doi: 10.1007/s10965-020-2021-0.
- [39] A. Rodríguez-Galan, N. Paredes, and J. Puiggali, “Biodegradable polymers: new poly (ester amide) s derived from alpha-amino acids,” *Curr Trends Polym Sci*, vol. 5, pp. 41–51, 2000.
- [40] A. Rodríguez-Galan, L. Franco, and J. Puiggali, “Degradable Poly(ester amide)s for Biomedical Applications,” *Polymers*, vol. 3, no. 1, pp. 65–99, Dec. 2010, doi: 10.3390/polym3010065.
- [41] F. V. Borbolla-Jiménez *et al.*, “Films for Wound Healing Fabricated Using a Solvent Casting Technique,” *Pharmaceutics*, vol. 15, no. 7, p. 1914, Jul. 2023, doi: 10.3390/pharmaceutics15071914.
- [42] P. Anbukarasu, D. Sauvageau, and A. Elias, “Tuning the properties of polyhydroxybutyrate films using acetic acid via solvent casting,” *Sci. Rep.*, vol. 5, no. 1, p. 17884, Dec. 2015, doi: 10.1038/srep17884.
- [43] Y. Zena *et al.*, “Essential characteristics improvement of metallic nanoparticles loaded carbohydrate polymeric films - A review,” *Int. J. Biol. Macromol.*, vol. 242, p. 124803, Jul. 2023, doi: 10.1016/j.ijbiomac.2023.124803.
- [44] E. Naseri and A. Ahmadi, “A review on wound dressings: Antimicrobial agents, biomaterials, fabrication techniques, and stimuli-responsive drug release,” *Eur. Polym. J.*, vol. 173, p. 111293, Jun. 2022, doi: 10.1016/j.eurpolymj.2022.111293.
- [45] A. Haider, S. Haider, and I.-K. Kang, “A comprehensive review

- summarizing the effect of electrospinning parameters and potential applications of nanofibers in biomedical and biotechnology,” *Arab. J. Chem.*, vol. 11, no. 8, pp. 1165–1188, Dec. 2018, doi: 10.1016/j.arabjc.2015.11.015.
- [46] “<http://polybiolab.ippt.pan.pl/research/electrospinning>,” <http://polybiolab.ippt.pan.pl/research/electrospinning>. [Online]. Available: <http://polybiolab.ippt.pan.pl/research/electrospinning>
- [47] J. Xue, T. Wu, Y. Dai, and Y. Xia, “Electrospinning and Electrospun Nanofibers: Methods, Materials, and Applications,” *Chem. Rev.*, vol. 119, no. 8, pp. 5298–5415, Apr. 2019, doi: 10.1021/acs.chemrev.8b00593.
- [48] T. J. Sill and H. A. von Recum, “Electrospinning: applications in drug delivery and tissue engineering,” *Biomaterials*, vol. 29, no. 13, pp. 1989–2006, May 2008, doi: 10.1016/j.biomaterials.2008.01.011.
- [49] A. Ghaderpour, Z. Hoseinkhani, R. Yarani, S. Mohammadiani, F. Amiri, and K. Mansouri, “Altering the characterization of nanofibers by changing the electrospinning parameters and their application in tissue engineering, drug delivery, and gene delivery systems,” *Polym. Adv. Technol.*, vol. 32, no. 5, pp. 1924–1950, May 2021, doi: 10.1002/pat.5242.
- [50] D. Mailley, A. Hébraud, and G. Schlatter, “A Review on the Impact of Humidity during Electrospinning: From the Nanofiber Structure Engineering to the Applications,” *Macromol. Mater. Eng.*, vol. 306, no. 7, p. 2100115, Jul. 2021, doi: 10.1002/mame.202100115.
- [51] B. Araldi Da Silva, R. De Sousa Cunha, A. Valério, A. De Noni Junior, D. Hotza, and S. Y. Gómez González, “Electrospinning of cellulose using ionic liquids: An overview on processing and applications,” *Eur. Polym. J.*, vol. 147, p. 110283, Mar. 2021, doi: 10.1016/j.eurpolymj.2021.110283.
- [52] H. Maleki, B. Azimi, S. Ismaeilimoghadam, and S. Danti, “Poly(lactic acid)-Based Electrospun Fibrous Structures for Biomedical Applications,” *Appl. Sci.*, vol. 12, no. 6, p. 3192, Mar. 2022, doi: 10.3390/app12063192.
- [53] S. Jiang, Q. Jin, and S. Agarwal, “Template Assisted Change in Morphology from Particles to Nanofibers by Side-by-Side Electrospinning of Block Copolymers,” *Macromol. Mater. Eng.*, vol. 299, no. 11, pp. 1298–1305, Nov. 2014, doi: 10.1002/mame.201400059.
- [54] H. Jiang, L. Wang, and K. Zhu, “Coaxial electrospinning for encapsulation and controlled release of fragile water-soluble bioactive agents,” *J. Controlled Release*, vol. 193, pp. 296–303, Nov. 2014, doi: 10.1016/j.jconrel.2014.04.025.

Acknowledgments

I want to express my deep gratitude to several individuals and aspects of my life that have profoundly influenced my academic journey and the completion of this thesis.

Professor Ana Clotilde, my guiding light during the internship at the University of Coimbra. Her unwavering support, kindness, and trust were indispensable, especially as I navigated a challenging and unfamiliar topic for my thesis.

Pedro Nunes, my mentor, whose meticulous and professional guidance not only introduced me to this field but also transformed my understanding. Pedro has been a significant influence, and I am endlessly thankful for the wisdom he shared.

Professor Cristiana Corsi, my thesis supervisor at the University of Bologna, deserves my heartfelt appreciation for her continuous support and availability throughout the thesis process.

My family, in particular my father, my mother, and my brother, deserve a special acknowledgment for their unwavering support during my master's journey. Their encouragement was crucial, both in Cesena and during my transformative exchange year in Portugal.

My friends, particularly those I connected with during my exchange year in Portugal, added vibrant colors to this chapter of my life. Despite initial fears, they made it the most incredible year of my life.

Jai, your constant presence has been a source of strength and friendship throughout these years. I am truly grateful for your unwavering support.

Life itself deserves a special mention for granting me the opportunity to live in Portugal, a deep experience that allowed me to discover myself more fully. That year stands out as the most incredible period of my life.

Finally, I want to express gratitude to myself for embarking on a journey that led me to study in three different countries, each presenting its unique set of challenges. Navigating through fears and overcoming insecurities demanded inner strength and courage. Recognizing and embracing this personal growth stands as an essential component of my transformative journey, and I am thankful for having embarked on this self-discovery.

Alessio